New Parameterization and Analysis for E6 Inspired 331 Model

Rena Çiftçi,[1] Abbas Kenan Çiftçi,[2] and Oleg Popov[3,4,*]

[1]*Department of Physics, Faculty of Science, Ege University, 35040 Bornova, Izmir, Türkiye*

[2]*Department of Physics, Faculty of Arts and Sciences, Izmir University of Economics, 35330 Balçova, Izmir, Türkiye*

[3]*Department of Biology, Shenzhen MSU-BIT University, 1, International University Park Road, Shenzhen 518172, China*

[4]*Department of Physics, Korea Advanced Institute of Science and Technology, 291 Daehak-ro, Yuseong-gu, Daejeon 34141, Republic of Korea*

Abstract

We present a new parameterization for $SU(3)_C \times SU(3)_L \times U(1)_X$ extension of the Standard Model, which is inspired by E_6 symmetry. The new setup predicts all Cabibbo-Kobayashi-Maskawa mixing angles and quark masses, a total of nine observable variables, within 1–3 standard deviations of the experimental values with a minimum number of input parameters. A detailed numerical analysis and correlations between input parameters and predicted quantities are presented. The best global fit benchmark point corresponds to $\chi^2 \approx 0.7$ with $\forall\sigma < 0.6$. The advantages of the new parameterization and future prospects are discussed as well.

Keywords: 331 model, quark mass, CKM, mixing, parameterization, E6
DOI: 10.31526/LHEP.2024.481

1. INTRODUCTION

In spite of its effectiveness in accurately explaining electromagnetic, strong, and weak interactions, the Standard Model (SM) has significant unresolved issues, such as the large mass spectrum and hierarchy of fermions, the small quark mixing angles, the existence of three fermion families, CP violation, the origin of neutrino masses, and dark matter. Many extensions of SM have been investigated to address some of these issues. The so-called 331 models are one of the simplest extensions, which modify the electroweak gauge group of SM from $SU(3)_C \otimes SU(2)_L \otimes U(1)_Y$ to a $SU(3)_C \otimes SU(3)_L \otimes U(1)_X$ symmetry (331, hereafter). In the beginning, these models were presented as a natural explanation for the observed number of fermion families in nature. Various variants of the 331 model have been studied in detail to date. This model can be made anomaly-free in various ways. The 331 model can be made anomaly-free within the family as in the SM, or in other variants, it can be made anomaly-free by using all 3 families. The second approach is very attractive as it may be a natural explanation for the number of families being 3 in the SM.

The 331-based model has been the focus of many studies and is motivated by solving problems in various phenomenological applications. For instance, works on a 331 model have been applied in flavor physics [1, 2, 3, 4], neutrino mass generation [5, 6], and other phenomenological issues [7, 8, 9, 10, 11, 12, 13, 14, 15, 16]. Furthermore, in view of the well-known W boson mass anomaly, which was reported recently by the Collider Detector at Fermilab (CDF) Collaboration taken at the Tevatron particle accelerator [17], a possible connection between W mass anomaly and the super-symmetric variation of the 331 model was examined [18]. For recent works on 331 models please refer to [19, 20, 21, 22]. On the other hand, 331-based models can be viewed as a precursor to grand unification models at high energy scales [23, 24, 25]. Finally, the 3311 model, which is an extended variation of the 331 model, has been investigated in conjunction with dark matter candidates and neutrino mass generation mechanism [26, 27, 28, 29].

The mass spectrum and the mixing of quarks are one of the important unsolved problems of particle physics. Experimental values of quark masses at the scale of mass of Z boson are listed as $m_d = 2.67 \pm 0.19\,\text{MeV}$, $m_s = 53.16 \pm 4.61\,\text{MeV}$, $m_b = 2.839 \pm 0.026\,\text{GeV}$, $m_u = 1.23 \pm 0.21\,\text{MeV}$, $m_c = 620 \pm 17\,\text{MeV}$, $m_t = 168.26 \pm 0.75\,\text{GeV}$ [30], whereas masses in [31] are given at different scales. Experimental limits [30] at $M_Z = 91.1876\,\text{GeV}$ scale of Cabibbo-Kobayashi-Maskawa (CKM) mixing matrix are

$$V_{\text{CKM}}^{W} = \begin{pmatrix} |V_{ud}| & |V_{us}| & |V_{ub}| \\ |V_{cd}| & |V_{cs}| & |V_{cb}| \\ |V_{td}| & |V_{ts}| & |V_{tb}| \end{pmatrix} = \begin{pmatrix} 0.97401 \pm 0.00011 & 0.22650 \pm 0.00048 & 0.00361^{+0.00011}_{-0.00009} \\ 0.22636 \pm 0.00048 & 0.97320 \pm 0.00011 & 0.04053^{+0.00083}_{-0.00061} \\ 0.00854^{+0.00023}_{-0.00016} & 0.03978^{+0.00082}_{-0.00060} & 0.999172^{+0.000024}_{-0.000035} \end{pmatrix}. \quad (1)$$

There are a number of attempts to explain masses and the relation of CKM matrix elements to them. Somehow parameterization of CKM quark and Pontecorvo-Maki-Nakagawa-Sakata (PMNS) neutrino mixing matrices have always been very intriguing problems of particle physics. For example, Wolfenstein parameterization and its various extensions [32, 33] have gotten some attention. Triminimal and tribimaximal approaches have been also very popular parameterization methods [32, 33, 34, 35, 36]. A number of particle physicists used exponential [32, 33], recursive [37], rephasing invariants [38] parameterizations and unified pameterization of quarks and lepton matrices [36, 39] and also parameterization involving eigenvalues [40] can be listed for the mixing matrix parameterization. However, this incomplete list of parameterizations does not try to solve mixing in conjunction with mass hierarchy. Recent work on CKM and PMNS parametrization is given in [41].

The democratic mass matrix (DMM) approach has been proposed mainly by H. Fritzsch [42, 43, 44, 45, 46] for the SM. In this approach, all quarks with the same quantum number behave equally under weak interaction in the up and down sectors, and they are indistinguishable before the symmetry

*Corresponding author: opopo001@ucr.edu

breaking:

$$\mathcal{M}_u^0 = h_u \begin{pmatrix} 1 & 1 & 1 \\ 1 & 1 & 1 \\ 1 & 1 & 1 \end{pmatrix}, \tag{2}$$

$$\mathcal{M}_d^0 = h_d \begin{pmatrix} 1 & 1 & 1 \\ 1 & 1 & 1 \\ 1 & 1 & 1 \end{pmatrix}. \tag{3}$$

Since there is only one Higgs field in the SM, $h_u = h_d$ is expected. In this case, it is naturally expected that $m_b \cong m_t$. The reason why the masses of these quarks are not close to each other may be due to the fact that the SM is not the last and most basic theory. To circumvent this, it was proposed to extend the SM to 4 families [47, 48, 49, 50, 51]. As can be easily seen in this model, the mass difference between the t and b quarks can be explained inherently. However, ATLAS and CMS data excluded the 4th family [52, 53]. Although the 4th family vector quark is not excluded by the experimental data, this deviates from the V-A theory, the natural approach of the SM.

In this paper, we will apply the DMM scheme to the anomaly-free 331 model for a single family because it is closer to the SM approach. The 331 model being among the subgroups of E_6 [54, 55, 56] grand unification theory is another advantage of this model. One of the most important features of the E_6 inspired 331 model is the prediction of 3 different Higgs fields. This means that the up-quark and the down-quark interact with different Higgs fields. The last Higgs contributes to the mass of the heavy isosinglet quarks. With the DMM scheme, it will show that the quark masses and the CKM mixing angles of the SM can be obtained naturally in agreement with the most recent experimental data.

The extension of the $SU(3)_L \otimes U(1)_X$ flavor group with possible fermion and Higgs-boson representations has been investigated [57]. Some have studied these extensions as indistinguishable duplicates of a family as in SM [54, 58, 59, 60, 61, 62, 63, 64, 65, 66, 67, 68, 69, 70], while others have looked at them as a multifamily construct [8, 71, 72, 73, 74, 75, 76, 77, 78, 79], implying a natural solution to the problem of SM fermion family number [7, 11, 80, 81, 82]. Many models lead to flavor-changing neutral currents [54, 59, 60, 62, 63, 65, 66, 69], right-handed currents at low scales [69], violation of quark-lepton universality [58, 65, 66, 83, 84], and flavor anomalies [2]. For instance, some models studied in [8, 71, 73, 74, 75, 76, 77, 78, 79] lead to physical inconsistencies which rule them out. Meanwhile, this is in agreement with the SM phenomenology, with the 3 quark and 3 lepton families, and the anomaly of the model is eliminated by the addition of quarks carrying exotic electric charges. The model in [7, 11, 80, 81, 82] is also three-family and is in agreement with low energy phenomenology but does not contain exotic electrically charged fermions. In this study, the quark sector of well-known E_6 inspired $SU(3)_C \otimes SU(3)_L \otimes U(1)_X$ model is considered. It can be renamed in short as Variant-A of 331 model. Details of this variant are given in [85].

In this work, the Variant-A of 331 model is investigated in the light of DMM. The structure of the paper is as follows: Section 2 introduces the 331 model and its variations. The quark content of the Variant-A is presented. Then, the definition of the Higgs fields and new gauge bosons of the model and charged and neutral currents are given. DMM approach is applied to the Variant-A of 331 model. In Section 3, new parameterization of the Variant-A is defined. Numerical analysis and obtained correlation plots are presented in Section 4. Section 5 contains the results of the analysis, more specifically the input parameters and obtained observable variables for the three most relevant and important benchmark points. Section 6 discusses the features and prospects of the obtained results. Finally, Section 7 concludes the work.

2. 331 MODEL

As mentioned earlier, the $SU(3)_C \otimes SU(3)_L \otimes U(1)_X$ model is one of the minimal extensions of SM. Various submodels of this model studied earlier [85] contain no exotic electrically charged particles. Two types of these models are variants (A and B) [86, 87] that have no triangle anomalies in one family, and the other two are variants (C and D) [7, 72, 73, 81] that have no triangle anomalies in three families. In three-family models, one has different quantum numbers from the other two. Here, the electroweak gauge group is supposed to be $SU(3)_L \otimes U(1)_X \supset SU(2)_L \otimes U(1)_Y$. It is also assumed that left-handed quarks (color triplets) and left-handed leptons (color singlets) transform under the two basic representations of $SU(3)_L$ (3 and 3^*). The gauge boson sector is identical in all models, but they may diverge in their quark and lepton contents and scalar sector. In this paper, the quark sector of Variant-A of the one family model is considered. The field content of the model, given in the coming subsections, is assumed to be an IR particle content of the E_6 inspired and maximally broken down to $[SU(3)]^3 \to SU(3) \times SU(3) \times U(1)$ via a spontaneous symmetry breaking sequence. The current, 331 level, particle content is a chiral anomaly free per family, after integrating out heavier states of E_6. Furthermore, the gauge symmetry charges of the 331 particle content under the $SU(3) \times SU(3) \times U(1)$ symmetry are such that they match the charges of the $[SU(3)]^3$ before the symmetry breaking [85, 86, 87].

2.1. Quark and Lepton Contents of Variant-A

The quark structure for this model [85] is as follows:

$$\begin{array}{cccc} Q_L^\alpha = \begin{pmatrix} u_\alpha \\ d_\alpha \\ D_\alpha \end{pmatrix}_L & u_{\alpha L}^c & d_{\alpha L}^c & D_{\alpha L}^c, \\ \{3,3,0\} & \left\{3^*,1,-\frac{2}{3}\right\} & \left\{3^*,1,\frac{1}{3}\right\} & \left\{3^*,1,\frac{1}{3}\right\} \end{array} \tag{4}$$

where $\alpha = 1,2,3$ correspond to the three families. Numbers in parenthesis refer to ($SU(3)_C$, $SU(3)_L$, and $U(1)_X$) quantum numbers, where X arising in the electric charge generators of the gauge group is defined as

$$Q = \frac{1}{2}\lambda_{3L} + \frac{1}{2\sqrt{3}}\lambda_{8L} + XI_3, \tag{5}$$

where λ_{iL} ($i = 1, \ldots, 8$) are Gell-Mann matrices for $SU(3)_L$ and I_3 is the 3-dimensional identity matrix.

Including the lepton content and quantum numbers [85] given below, this model is anomaly-free:

$$\begin{array}{ccc} \psi_L^\alpha = \begin{pmatrix} e_\alpha^- \\ \nu_\alpha \\ N_{1\alpha}^0 \end{pmatrix}_L & \psi_{1L}^\alpha = \begin{pmatrix} E_\alpha^- \\ N_{2\alpha}^0 \\ N_{3\alpha}^0 \end{pmatrix}_L & \psi_{1L}^\alpha = \begin{pmatrix} N_{4\alpha}^0 \\ E_\alpha^+ \\ e_\alpha^+ \end{pmatrix}_L. \\ \left\{1,3^*,-\frac{1}{3}\right\} & \left\{1,3^*,-\frac{1}{3}\right\} & \left\{1,3^*,\frac{2}{3}\right\} \end{array} \tag{6}$$

2.2. Higgs and New Gauge Bosons

The model contains three Higgs fields, which are

$$\phi_1 = \begin{pmatrix} \phi_1^- \\ \phi_1^0 \\ \phi_1'^0 \end{pmatrix} \quad \phi_2 = \begin{pmatrix} \phi_2^- \\ \phi_2^0 \\ \phi_2'^0 \end{pmatrix} \quad \phi_3 = \begin{pmatrix} \phi_3^0 \\ \phi_3^+ \\ \phi_3'^+ \end{pmatrix} \tag{7}$$
$$\left\{1, 3^*, -\tfrac{1}{3}\right\} \quad \left\{1, 3^*, -\tfrac{1}{3}\right\} \quad \left\{1, 3^*, \tfrac{2}{3}\right\}$$

with Vacuum Expectation Values (VEV):

$$\begin{aligned} \langle \phi_1 \rangle &= (0, 0, M)^T, \\ \langle \phi_2 \rangle &= \left(0, \frac{\eta}{\sqrt{2}}, 0\right)^T, \\ \langle \phi_3 \rangle &= \left(\frac{\eta'}{\sqrt{2}}, 0, 0\right)^T, \end{aligned} \tag{8}$$

where $\eta \sim 250\,\text{GeV}$ ($\eta' = \eta$ can be taken for simplicity).

In addition, this model has a total of 17 gauge bosons. One of the gauge fields is the gauge boson associated with $U(1)_X$. Eight of them are $SU(3)_C$ associated gauge bosons.The gauge fields of the electroweak sector can be listed as $W^\pm$, $W'^\pm$, W'^0, and $\bar{W}'^0$ with mass for charged currents, and Z and Z' for the neutral currents, which are also massive and uncharged. The masses of the new bosons are proportionate to the symmetry breaking scale of the model, in the order of a few TeV. The masses of the gauge bosons of the electroweak sector can be found using the following expressions:

$$m_{W^\pm}^2 = \frac{g^2}{4}\left(\eta^2 + \eta'^2\right), \tag{9a}$$

$$m_Z^2 = \frac{m_{W^\pm}^2}{C_W^2}, \tag{9b}$$

$$m_{W'^\pm}^2 = \frac{g^2}{4}\left(2M^2 + \eta'^2\right), \tag{9c}$$

$$m_{W'^0(\bar{W}'^0)}^2 = \frac{g^2}{4}\left(2M^2 + \eta^2\right), \tag{9d}$$

$$m_{Z'}^2 = \frac{g^2}{4\left(3 - 4S_W^2\right)}\left[8C_W^2 M^2 + \frac{\eta^2}{C_W^2} + \frac{\eta^2\left(1 - 2S_W^2\right)^2}{C_W^2}\right], \tag{9e}$$

where $C_W = \cos\theta_W$ and $S_W = \sin\theta_W$ are the cosine and sine of the electroweak mixing angle (a.k.a. Weinberg angle), respectively, with the experimental value of $S_W^2 = 0.23122$. It should be emphasized that, in addition to the SM, there are five new gauge bosons, which may lie within the detection limits of the Large Hadron Collider (LHC), as we assume their masses to be in the order of a few TeV. Constraints on the masses of these particles have been identified by searches of 331 vector bosons from LHC proton collision data [88] and deep learning analysis on LHC data [89]. The corresponding limits on the Z' gauge boson of the 331 model are $m_{Z'} \geq 3.7\,\text{TeV}$ [88] and $m_{Z'} \geq 4.0\,\text{TeV}$ [89]. In fact, the common feature of many models obtained by extending the SM is the participation of extra heavy gauge bosons [31], the charged ones usually denoted by W'. In the LHC, W' bosons would be observed through production of fermion or electroweak boson pairs resonantly. The most extensively considered signature contains a high-energy electron or muon and large lost transverse energy. Assuming that these new bosons couple with fermions in the SM, restrictive constraints on the mass of W' are obtained as $M_{W'} > 6\,\text{TeV}$ at 95% CL [90]. Although this limitation does not directly apply to our model, it gives a sense of the masses of the $W'^\pm$ and W'^0 bosons.

Charged currents in this model are as follows:

$$\begin{aligned} \mathcal{L}_{CC} = -\frac{g}{\sqrt{2}}\Big[&\bar{\nu}_L^\alpha \gamma^\mu e_L^\alpha W_\mu^+ + \bar{N}_L^\alpha \gamma^\mu e_L^\alpha W_\mu'^+ \\ &+ \bar{\nu}_L^\alpha \gamma^\mu N_L^\alpha W_\mu'^0 + \bar{u}_{\alpha L}\gamma^\mu d_{\alpha L} W_\mu^+ \\ &+ \bar{u}_{\alpha L}\gamma^\mu D_{\alpha L} W_\mu'^+ - \bar{D}_{\alpha L}\gamma^\mu d_{\alpha L} W_\mu'^0 + \text{h.c.}\Big], \end{aligned} \tag{10}$$

and neutral currents are given as follows [86]:

$$\begin{aligned} \mathcal{L}^{NC} &= -\frac{g}{2C_W}\sum_f \left[\bar{f}\gamma^\mu\left(g_V' + g_A'\gamma^5\right) f Z_\mu'\right] \\ &= \frac{g'}{\sqrt{3}}\sum_f \bar{f}\gamma_\mu\left[T_W Q_f - \text{Diag}\left(S_{2W}^{-1}, T_{2W}^{-1}, -T_W^{-1}\right) P_L\right] f Z'^\mu, \end{aligned} \tag{11}$$

where f represents leptons and quarks; g, g_V', and g_A' are the coupling constants of $SU(3)_L$. Also, $T_W = \tan\theta_W$, $T_{2W} = \tan(2\theta_W)$ and $S_{2W} = \sin(2\theta_W)$ are used in equation (11).

As can be seen from the above expressions, W'^+ and W'^- gauge bosons provide transitions between up-sector quarks and new isosinglet D quarks, while W'^0 and $\bar{W}'^0$ gauge bosons mediate the interactions of SM down-sector quarks and new isosinglet quarks. Even though currents of W'^0 and $\bar{W}'^0$ gauge bosons are given as part of the charged current sector, they can be interpreted as off-diagonal neutral currents due to their zero electric charge.

2.3. Democratic Approach to the Quark Sector of the 331 Model

The democratic mass matrix (DMM) approach was developed by H. Harari and H. Fritzsch [42, 43, 44, 45, 46] to solve the mass hierarchy and mixing problems. To predict all the masses and mixings, a number of papers were published, in which DMM was applied to four family SM [47, 48]. Later, the SM type fourth family fermions were excluded by ATLAS and CMS data [52, 53]. As a consequence, if the DMM approach is correct, it will be inevitably applied to an extension of the SM. DMM assumes that Yukawa coupling constants should be approximately the same in the weak interaction Lagrangian. When the mass eigenstates are turned on, fermions gain different masses [49, 50, 51].

When applying the DMM approach to the Variant-A of 331 model, two different basis are defined: $SU(3)_L \otimes U(1)_X$ symmetry basis, labeled with superscript "(0)" as in $f^{(0)}$ and the mass basis labeled without superscript as in f, where f stands for any fermion particle. Before the electroweak spontaneous

symmetry breaking, quarks are grouped as follows:

$$\begin{pmatrix} u^{(0)} \\ d^{(0)} \\ D^{(0)} \end{pmatrix}_L , \quad u_L^{c(0)}, \quad d_L^{c(0)}, \quad D_L^{c(0)}, \tag{12a}$$

$$\begin{pmatrix} c^{(0)} \\ s^{(0)} \\ S^{(0)} \end{pmatrix}_L , \quad c_L^{c(0)}, \quad s_L^{c(0)}, \quad S_L^{c(0)}, \tag{12b}$$

$$\begin{pmatrix} t^{(0)} \\ b^{(0)} \\ B^{(0)} \end{pmatrix}_L , \quad t_L^{c(0)}, \quad b_L^{c(0)}, \quad B_L^{c(0)}. \tag{12c}$$

In the one-family case, all bases are equal. The Lagrangian with the quark Yukawa terms for the only one-family case can be written as follows:

$$\begin{aligned} \mathcal{L}_y^Q = Q_L^T C \, (&a_u \phi_3 u_L^c + a_d \phi_2 d_L^c + a_D \phi_1 D_L^c \\ &+ a_{dD} \phi_2 D_L^c + a_{Dd} \phi_1 d_L^c) + \text{h.c.}, \end{aligned} \tag{13}$$

where a_u, a_d, a_D, a_{dD}, and a_{Dd} are Yukawa couplings in the $SU(3)_L \otimes U(1)_X$ basis and C is the charge conjugate operator.

In this case, we obtain a mass term for the up-quark sector:

$$m_u^0 = a_u \frac{\eta^u}{\sqrt{2}} \quad \left(\eta^u = \eta^d = \eta \text{ is taken for simplicity}\right), \tag{14}$$

and a mass term for the down-quark sector is given as follows:

$$m_{dD}^0 = \begin{pmatrix} a_d \eta^d/\sqrt{2} & \varepsilon a_d \eta^d/\sqrt{2} \\ \varepsilon a_D \eta^D/\sqrt{2} & a_D \eta^D/\sqrt{2} \end{pmatrix}, \tag{15}$$

where ε is chosen very close to one, and εa_d corresponds to the a_{dD} and εa_D corresponds to the a_{Dd}.

In order to obtain mass eigenvalues, we need to diagonalize the above mass matrix. This is done in [91] to demonstrate that this approach gives correct t and b quark masses in the one-family case.

Now, we can write the three-family quark Yukawa Lagrangian in the $SU(3)_L \otimes U(1)_X$ basis:

$$\begin{aligned} \mathcal{L}_y^Q = \sum_{i,j}^{3} Q_{iL}^T C \Big(&a_{u_i u_j} \phi_3 u_{jL}^c + a_{d_i d_j} \phi_2 d_{jL}^c + a_{D_i D_j} \phi_1 D_{jL}^c \\ &+ \varepsilon a_{d_i D_j} \phi_2 D_{jL}^c + \varepsilon a_{D_i d_j} \phi_1 d_{jL}^c \Big) + \text{h.c.}, \end{aligned} \tag{16}$$

where $a_{u_i u_j}$, $a_{d_i d_j}$, $a_{D_i D_j}$, $a_{d_i D_j}$, and $a_{D_i d_j}$ are Yukawa couplings for the three-family case.

3. MODEL PARAMETERIZATION

One can form the most general mass matrix for up and down-sector quarks from equation (16). To determine the further structure of the mass matrix, we will break symmetries from higher mass quarks to lower mass ones as proposed in [45]. It is convenient to write a 6×6 down-sector mass matrix as a 2×2 matrix similar to equation (15) in terms of 3×3 sub matrices. When $\varepsilon = 1$, this 2×2 matrix has scaling and Z_2 symmetries from right and left, respectively. Here, only the symmetry breaking parameter is ε. When $\varepsilon = 1$, only the isosinglet D quark matrix takes a value and other 3×3 becomes zero. Symmetry can be broken by deviating ε from one slightly. In that case, the down-sector matrix gains a value in addition to the isosinglet sector matrix. With the help of mass of t quark, it is possible to determine $\frac{a_u \eta^u}{\sqrt{2}}$ as 56.5 GeV. Also, it is possible to choose $\frac{a_d \eta^d}{\sqrt{2}} = \frac{a_u \eta^u}{\sqrt{2}}$. In that case, $\varepsilon = 1.008$ gives us a second eigenvalue equal to roughly $\frac{1}{3}$ of the mass of b quark.

Consequently, effective mass matrix for down sector with $a_d = a_s = a_b$ is obtained equivalent to equation (3) with effective $h_d \approx 0.905$. This matrix has permutation group of three elements, Z_3, from left and right. Obviously, only the heaviest quark (b quark) gains mass with this symmetry. In order to obtain mass for the next heavy quark (s quark), the permutation symmetry of three elements should be broken into Z_2 with an introduction of deviations as follows:

$$\mathcal{M}_d^0 = h_d \begin{pmatrix} 1 & 1 & 1+\beta_d \\ 1 & 1 & 1+\beta_d \\ 1+\beta_d & 1+\beta_d & 1+4\beta_d \end{pmatrix}. \tag{17}$$

This will leave d quark massless. To break Z_2 symmetry, one should introduce new deviations. This deviation is parameterized with γ_d. The structure of parameterization related to γ should be chosen to satisfy experimental mass hierarchy and CKM angles.

As was mentioned earlier, the democratic form of all quark mass matrices is broken via a small deviation, represented by β and γ parameters. Furthermore, the form of deviation is identical for up, down, and heavy down type isosinglet quarks. There are two reasons for that. First, since there is no any experimental evidence showing that up- and down-quark sectors behave differently under weak interactions, breaking patterns should be universal in three matrices for different flavors. Second, if up and down type quarks have different breaking patterns, the CKM mixing matrix would deviate from unity matrix (as should be in SM) greatly. Besides that, the simplicity of the constructed model was another important property of the mass matrix pattern. These arguments lead to the parameterization pattern used in the present DMM model parameterization approach. Mass matrices for up, down, and heavy down type isosinglet quarks are as follows:

$$\mathcal{M}_u^0 = \frac{a_u \eta^u}{\sqrt{2}} \begin{pmatrix} 1+\gamma_u & 1 & 1-\frac{9}{2}\gamma_u+\beta_u \\ 1 & 1-2\gamma_u & 1+3\gamma_u+\beta_u \\ 1-\frac{9}{2}\gamma_u+\beta_u & 1+3\gamma_u+\beta_u & 1+4\beta_u \end{pmatrix}, \tag{18a}$$

$$\mathcal{M}_d^0 = \frac{a_d \eta^d}{\sqrt{2}} \begin{pmatrix} 1+\gamma_d & 1 & 1-\frac{9}{2}\gamma_d+\beta_d \\ 1 & 1-2\gamma_d & 1+3\gamma_d+\beta_d \\ 1-\frac{9}{2}\gamma_d+\beta_d & 1+3\gamma_d+\beta_d & 1+4\beta_d \end{pmatrix}, \tag{18b}$$

$$\mathcal{M}_D^0 = \frac{a_D \eta^D}{\sqrt{2}} \begin{pmatrix} 1+\gamma_D & 1 & 1-\frac{9}{2}\gamma_D+\beta_D \\ 1 & 1-2\gamma_D & 1+3\gamma_D+\beta_D \\ 1-\frac{9}{2}\gamma_D+\beta_D & 1+3\gamma_D+\beta_D & 1+4\beta_D \end{pmatrix}. \tag{18c}$$

However, down-sector quarks and isosinglet down type quarks are further mixed according to equation (16):

$$\mathcal{M}_{dD}^0 = \begin{pmatrix} \mathcal{M}_d^0 & \varepsilon_d \mathcal{M}_d^0 \\ \varepsilon_d \mathcal{M}_D^0 & \mathcal{M}_D^0 \end{pmatrix} = \begin{pmatrix} a_{d_i d_j} \eta/\sqrt{2} & a_{d_i D_j} \eta/\sqrt{2} \\ a_{D_i d_j} M & a_{D_i D_j} M \end{pmatrix}. \tag{19}$$

Yukawa couplings in equation (16) correspond to matrices given in equations (18a), (18b), (18c), and (19). The relation of elements of submatrices of (6×6) matrix to the Yukawa couplings is given in detail in equation (19). For the complete form

of the up- and down-quark mass matrices and the relation between Yukawa couplings and the model parameterization parameters ($\beta_{u,d,D}$ and $\gamma_{u,d,D}$), please refer to Appendix B.

Masses of down SM and Beyond Standard Model (BSM) isosinglet quarks are obtained by diagonalizing $\mathcal{M}^0_{dD}$ 6 by 6 mass matrix. This mass matrix can be diagonalized via a 6 by 6 unitary matrix U_{dD}, whereas masses of up-sector quarks are obtained by diagonalizing $\mathcal{M}^0_u$ mass matrix with a 3 by 3 unitary matrix U_u. Analogous 3 by 3 mixing matrices, U_d and U_D, for down type SM and heavy BSM quarks are defined as unitary matrices that diagonalize d and D blocks of the $\mathcal{M}^0_{dD}$ given in equation (19), respectively. For the sake of simplicity, the phases are considered as zero hereafter. Therefore, diagonalizing matrices will be real orthogonal matrices.

V^W_{CKM}, $V^{W'^{\pm}}$, and $V^{W'^0}$ mixing matrices correspond to the W SM electroweak gauge boson, while $W'^{\pm}$ and W'^0 are BSM heavy gauge bosons, respectively. These mixing matrices are defined via a combination of 3 by 3 diagonalizing matrices U_u, U_d, and U_D, mentioned earlier, and are given as

$$V^W_{\text{CKM}} = U_u U_d^T = \begin{pmatrix} V_{ud} & V_{us} & V_{ub} \\ V_{cd} & V_{cs} & V_{cb} \\ V_{td} & V_{ts} & V_{tb} \end{pmatrix}, \tag{20a}$$

$$V^{W'^{\pm}} = U_D U_u^T = \begin{pmatrix} V_{Du} & V_{Dc} & V_{Dt} \\ V_{Su} & V_{Sc} & V_{St} \\ V_{Bu} & V_{Bc} & V_{Bt} \end{pmatrix}, \tag{20b}$$

$$V^{W'^0} = U_D U_d^T = \begin{pmatrix} V_{Dd} & V_{Ds} & V_{Db} \\ V_{Sd} & V_{Ss} & V_{Sb} \\ V_{Bd} & V_{Bs} & V_{Bb} \end{pmatrix}. \tag{20c}$$

These matrices can be parameterized with three mixing angles and one phase angle:

$$V = \begin{pmatrix} c_{12}c_{13} & s_{12}c_{13} & s_{13}e^{-i\delta} \\ -s_{12}c_{23} - c_{12}s_{23}s_{13}e^{i\delta} & c_{12}c_{23} - s_{12}s_{23}s_{13}e^{i\delta} & s_{23}c_{13} \\ s_{12}s_{23} - c_{12}c_{23}s_{13}e^{i\delta} & -c_{12}s_{23} - s_{12}c_{23}s_{13}e^{i\delta} & c_{23}c_{13} \end{pmatrix}, \tag{21}$$

where $c_{ij} \equiv \cos\theta_{ij}$, $s_{ij} \equiv \sin\theta_{ij}$; the angles θ_{ij} are mixing angles, and δ is the CP violating phase angle (its contribution has not been considered in this study).

Extended CKM matrices (3×6) for V^W_{CKM} and $V^{W'^{\pm}}$ can be obtained using U_{dD}, mixing matrix of the 6 by 6 extended down-quark sector. The extended CKM matrix therefore, will give the interactions between 3 up type SM quarks and 6 (3 SM and 3 BSM) down type quarks. More details on this approach and quark unitarity arguments are included in Appendix C. In the further numerical analysis, for the simplicity purposes, the simplified (3×3) CKM approach will be employed.

4. NUMERICAL ANALYSIS

We perform a numerical scan over all parameter regions (7 input parameters, for details, see Table 1), first by randomly scanning over large parameter regions, and then by performing a close neighborhood scan over specific regions in order to find a global minimum with higher precision. After making numerical scans, we analyze the correlation between different input parameters, distinctive input parameters, and predicted observable variables, as well as between various output observable variables. The correlations presented below will increase the predictive power of the model and assist in probing the model in the current and future phenomenological experiments. Given further are the most striking correlations between these and attempt to explain the origin of correlations for some cases.

In order to obtain the results given in the benchmark points below, we used the following values for a and η (defined in Section 2.3) parameters

$$\frac{a_{u,d}\eta^{u,d}}{\sqrt{2}} = 56.5\,\text{GeV}, \tag{22a}$$

$$\frac{a_D\eta^D}{\sqrt{2}} = 3 \times 10^4\,\text{GeV}. \tag{22b}$$

These values were optimized in the analysis for the chosen parametrization. The scales in equation (22a) are not free, but rather constrained by SM quark masses. The change in these scales will affect the SM quark masses and CKM mixing angles, as well as BSM heavy quark masses. So, the scales in equation (22a) are subject to constraints from SM quark masses and CKM mixing angles. The scales in equation (22) play an important role, besides another significant parameter ε, while obtaining the light SM quark masses.

The scales in equation (22a) are fixed by the top mass and similarly of the scales between the two sectors and are treated as constants in the later analysis. The scale in equation (22b) has the strongest effect on the mass scale of the heavy BSM quarks, the masses of which are only subject to the lower bound constraints. Changing the scale in equation (22b) would mostly affect the heavy quarks and has very little effect on the SM observable variables. However, increasing the value in equation (22b) can be counterbalanced by deviating ε from 1. When the scale is increased, it is needed to change ε to keep SM down-sector quarks' masses in the experimental range. After a certain point, ε value does not change. In that case, it seems that there is no upper limit for the BSM scale. Therefore, the scale in equation (22b) is fixed in the further analysis.

The most apparent connected patterns between diverse input parameters are shown in Figure 1. As one may have noticed from Figure 1(a), there is an inverse correlation between β_u and β_d input parameters. Since β_u for up-sector behaves identically as does β_d for down-sector, these inverse correlation is originated from the CKM mixing angles. Figure 1(b) demonstrates the correlation between γ_u and γ_d, which exhibits an inverse correlation as well, analogously with the β's case. As a final example for the input parameters, Figure 1(c) depicts the direct correlation between input parameters that affect the down-sector mass eigenvalues. Other plots for different input parameters show weak or no correlated patterns, unlike the ones mentioned earlier.

The plots in Figure 2 demonstrate the important dependence of some observable variables on model input parameters. For instance, the plot in Figure 2(a) shows the direct dependence of m_u, the lightest eigenvalue of the up-quark sector, on its most sensitive input parameter, β_u. On the other hand, from Figure 2(b), one can see that there is an inverse nonlinear dependence of m_u on γ_u. Strong correlations are observed between β_u and m_c, as well as between β_u and m_t, direct linear and inverse linear, respectively, for m_c and m_t up-sector quark mass eigenvalues. As a consequence, there is a strong correlation between m_c and m_t (Figure 4(c)) and all up-sector eigenvalues show a strong dependence on the β_u input parameter for the model at hand. Regarding the down quark sector, an anal-

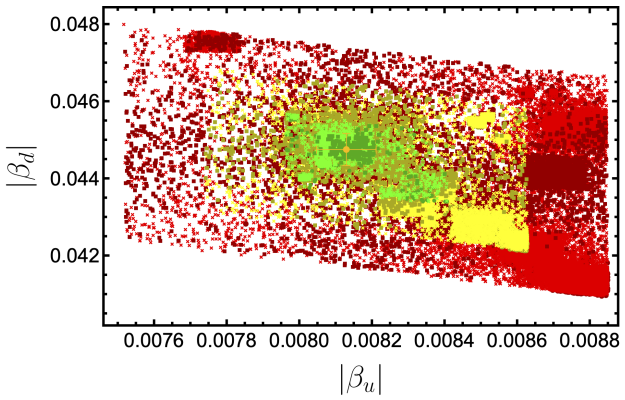

(a) β_u vs β_d correlation plot.

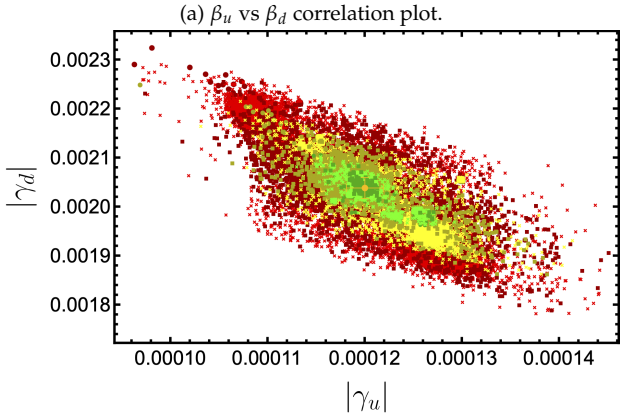

(b) γ_u vs γ_d correlation plot.

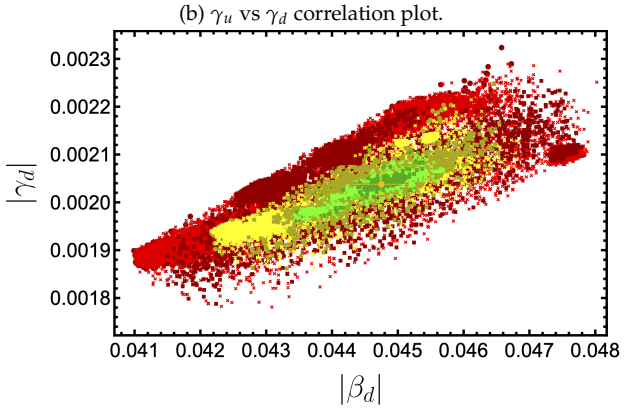

(c) β_d vs γ_d correlation plot.

FIGURE 1: Selected input correlation plots. Colors represent maximum standard deviation from experimental values. Green, yellow, and red colors stand for $\sigma_{\max} < 1$, 2, and 3, respectively, whereas squares, crosses, and discs correspond to $\langle\sigma\rangle / \sigma_{\max}$: 0–0.4, 0.4–0.6, and 0.6–1.0, respectively.

ogous correlation can be seen between β_d-m_s and β_d-sin($\theta_{23}^{\rm CKM}$) (Figures 2(e) and 2(f)), which exhibit proportional almost linear and direct-linear behavior, respectively. γ_d, similar to the situation in the up-sector in Figure 2(b), has the strongest influence on the m_d, lightest eigenvalue of the down-quark sector, Figure 2(g), with a direct behavior. Furthermore, the direct proportionality between m_d and γ_d can be seen from equation (18b), for which the lightest eigenvalue(m_d) approaches zero as γ_d goes to zero.

From the above analysis, it can be concluded that $\gamma_{u,d}$ has a noticeable influence on the lightest eigenvalue of its respective sector, whereas β_u affects all up-sector quark masses and β_d affects m_s and sin($\theta_{23}^{\rm CKM}$). This dependence of m_b on β_d is absent due to the mixing of SM down-quark sector with BSM heavy quarks.

The most striking correlations of the CKM mixing angles are observed for sin($\theta_{23}^{\rm CKM}$) mixing angle, which is directly proportional and completely determined by the two input parameters β_d and γ_d as shown in Figures 2(f) and 2(h). The other mixing angles exhibit more complex correlations with the input parameters.

Since BSM quarks are more massive than SM quarks there are no significant correlations between SM parameters and BSM observables, as seen from Figure 3. We have included only the plots for heavy D quark; the plots for S and B exhibit similar behavior with respect to β_u, γ_u, β_d, and γ_d parameters. However, M_D has a direct linear dependence on γ_D (Figure 3(f)), as well as, weaker dependence on β_D (Figure 3(e)). Analogous correlation is observed for M_S (Figures 3(h) and 3(g)). On the other hand, from Figures 3(i) and 3(j), one can see that strong correlations are observed between M_B and β_D, as well as between M_B and γ_D.

Plots in Figures 4(a), 4(b), and 4(c) demonstrate a direct, inverse, and inversely linear correlation between all three up-sector quark masses, respectively. This is an immediate consequence of the fact that all three strongly depend on the β_u input parameter Figures 2(a), 2(c), and 2(d).

Taking the $\gamma_u \ll \beta_u \ll 1$ limit in equation (18a), we obtain $m_u \propto 2\gamma_u \ll m_c, m_t$ and $m_t/m_c \approx 5.125 + 7.11806\beta_u + 2.25\beta_u^{-1}$,

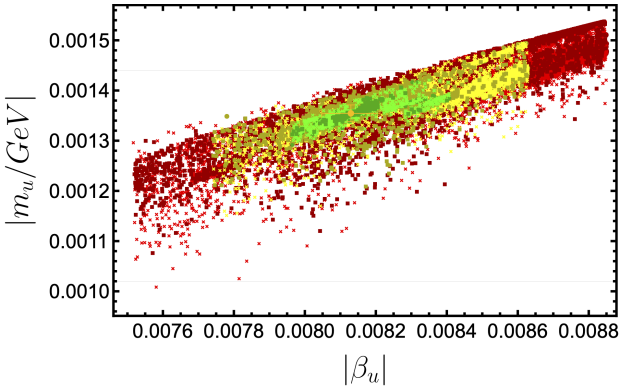

(a) β_u vs m_u correlation plot.

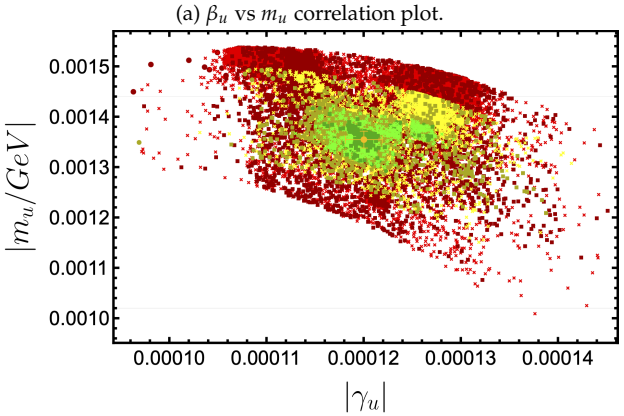

(b) γ_u vs m_u correlation plot.

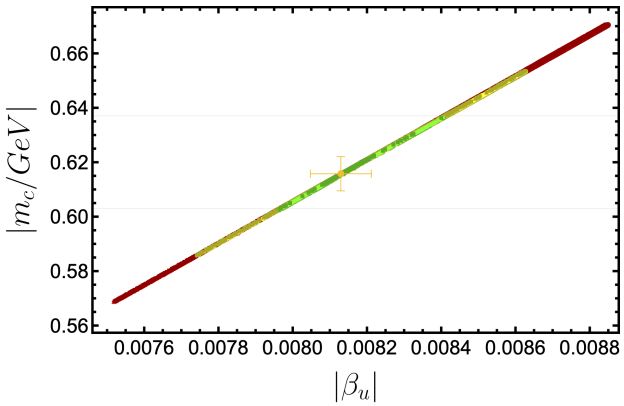

(c) β_u vs m_c correlation plot.

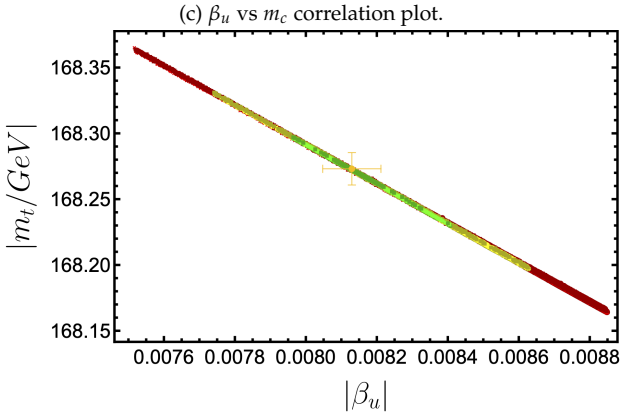

(d) β_u vs m_t correlation plot.

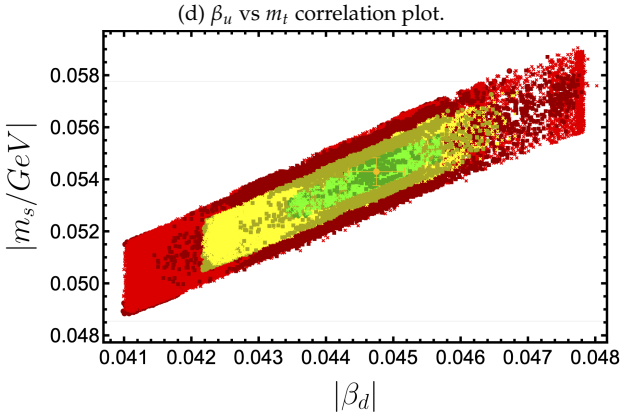

(e) β_d vs m_s correlation plot.

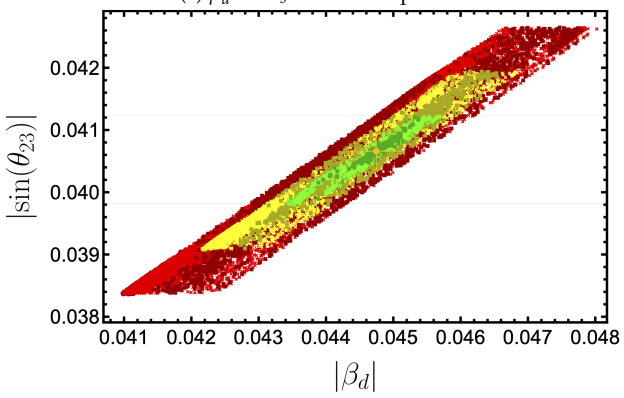

(f) β_d vs $\sin\left(\theta_{23}^{\mathrm{CKM}}\right)$ correlation plot.

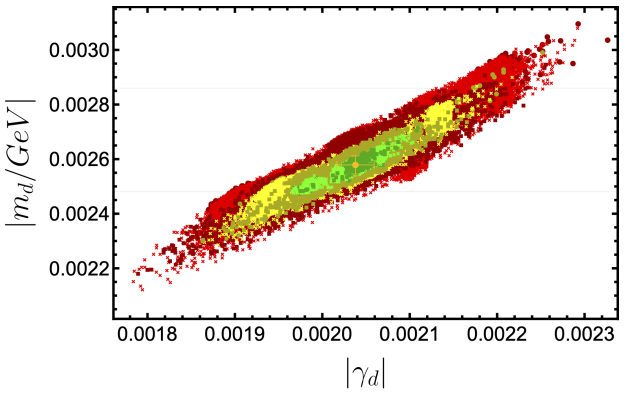

(g) γ_d vs m_d correlation plot.

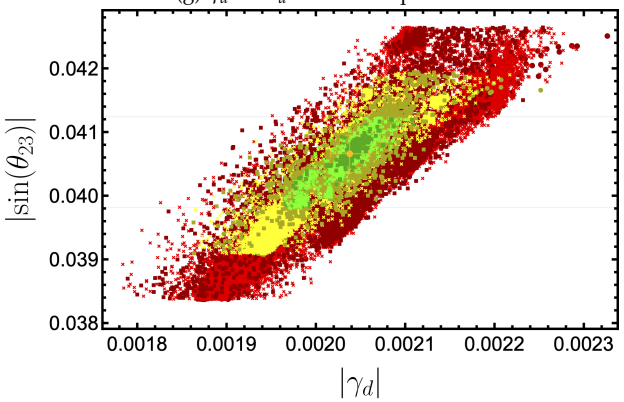

(h) γ_d vs $\sin\left(\theta_{23}^{\mathrm{CKM}}\right)$ correlation plot.

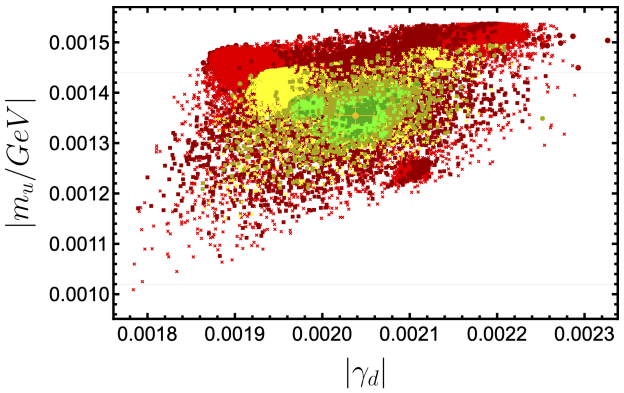

(i) γ_d vs m_u correlation plot.

FIGURE 2: Selected correlation plots between input parameters and observable variables. Grid lines indicate a one standard deviation region of the experimental data. Green, yellow, and red colors stand for $\sigma_{\max} < 1$, 2, and 3, respectively, whereas squares, crosses, and discs correspond to $\langle\sigma\rangle/\sigma_{\max}$: 0–0.4, 0.4–0.6, and 0.6–1.0, respectively.

which corresponds to the behavior $m_t \propto -m_c + \text{const.}$ (Figure 4(c)).

Figure 4(d) shows a correlation between the down-quark sector mass, m_s, and CKM mixing angle, $\sin(\theta_{23}^{\mathrm{CKM}})$. This can be seen from the direct linear dependence of $\sin(\theta_{23}^{\mathrm{CKM}})$ on β_d and γ_d, Figures 2(f) and 2(h), respectively. Similarly, m_s has a medium directly proportional dependence on β_d (Figure 2(e)), as well as, a weaker dependence on γ_d.

During the numerical analysis, in some cases, the obtained output observable variables may have been negative. In this case, the negative sign has been dropped, in view of the phases related argument made in the paragraph after equation (19).

5. RESULTS

In this section, the results of the model predictions are presented and elaborated on. This, E_6 motivated, variation of the 331 model predicts up- and down-quark masses, as well as CKM mixing angles for a total of seven input parameters. Up, down, and down type isosinglet quarks are controlled by two parameters each and one mixing parameter, ε, between light and heavy down-quarks. The input parameters for the three most relevant and important benchmark points are collected in Table 1. The first benchmark point (BP1) was obtained as a point with the smallest χ^2 of approximately 0.777, which has a maximum deviation from experimental results of 0.586 σ (refer to equation (23) for details). On the other hand, the second benchmark point (BP2) is defined as the point of a parameter scan with the smallest set of deviations for all nine observable variables at hand with a maximum deviation of $\sim$0.501 σ. As last, we give an average point for all data points obtained with $\forall\sigma_{\max} \leq 1$ as a third benchmark point (BP3), labeled as BP3$_{\langle\rangle}$ in Table 2, whereas the spread (error) of all points with $\forall\sigma_{\max} \leq 1$ is indicated as *Spread*. σ is defined as follows:

$$\sigma = \left| \frac{x_{\text{exp}} - x_{\text{th}}}{x_{\text{err}}} \right|, \tag{23}$$

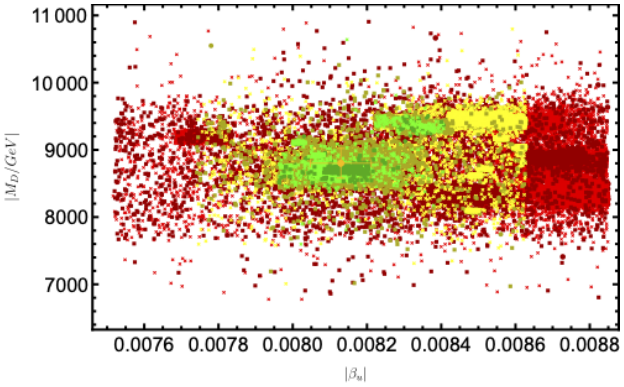

(a) M_D vs β_u correlation plot.

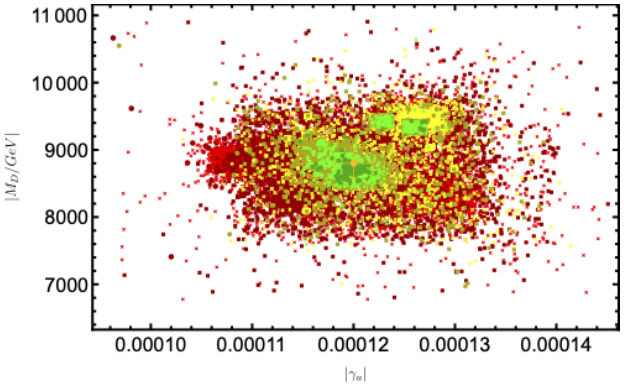

(b) M_D vs γ_u correlation plot.

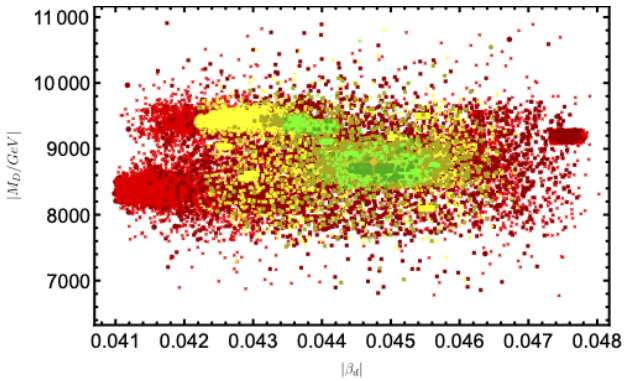

(c) M_D vs β_d correlation plot.

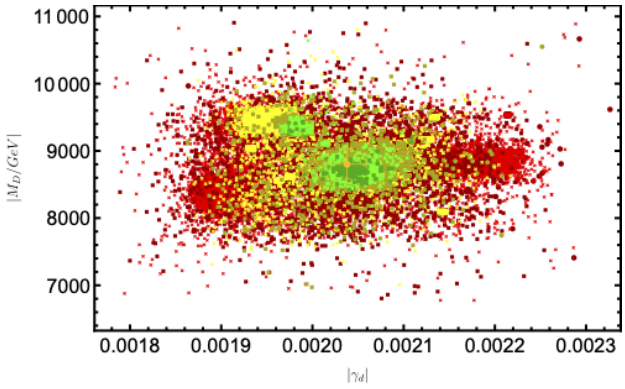

(d) M_D vs γ_d correlation plot.

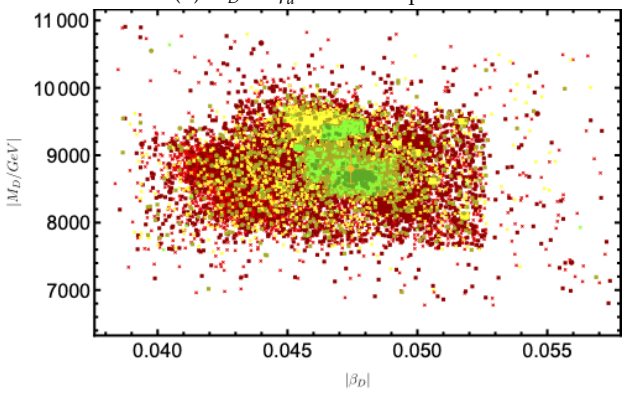

(e) M_D vs β_D correlation plot.

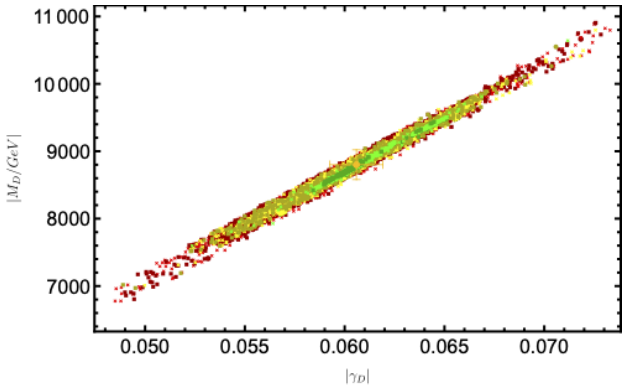

(f) M_D vs γ_D correlation plot.

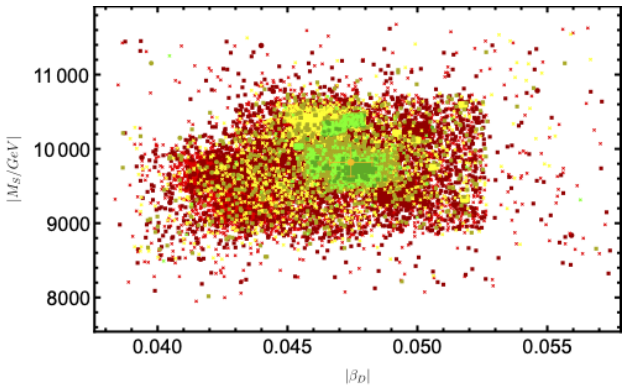

(g) M_S vs β_D correlation plot.

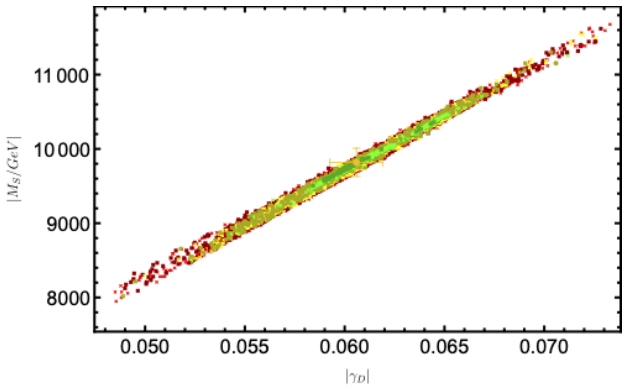

(h) M_S vs γ_D correlation plot.

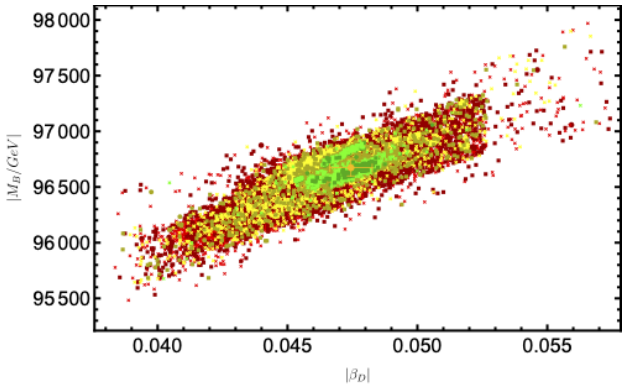

(i) M_B vs β_D correlation plot.

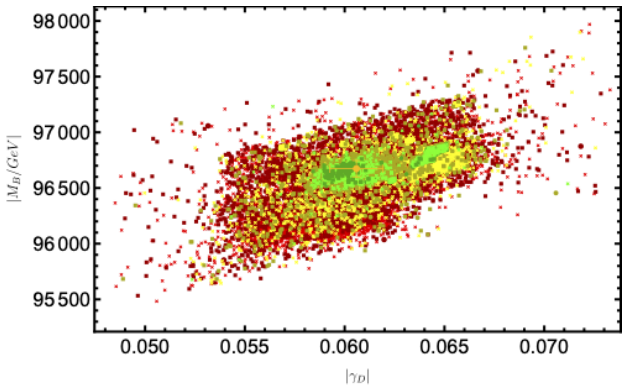

(j) M_B vs γ_D correlation plot.

FIGURE 3: Correlation plots between the BSM quark masses and quark sector parameters. Green, yellow, and red colors stand for $\sigma_{\max} < 1$, 2, and 3, respectively.

where x represents any of the observable variables from Table 2, *exp.* stands for the experimentally obtained value, *th* corresponds to the simulated value from the scan run, and lastly, *err.* means the error for the experimentally obtained value.

The parameter scan is very sensitive to the input parameters' value; therefore, we keep up to twenty decimal places. For a total of seven input parameters, the best result for χ^2 that was obtained is given in the 4th and 5th columns of Table 2 with $\chi^2 \approx 0.777$. As can be seen, the largest contribution to the χ^2 comes from m_u and m_d, whereas the second- and third-generation quark masses of up- and down-sectors contribute a much smaller error to the χ^2. Next, as a result of the search for the smallest combination of the deviations from the experimental values (2nd and 3rd columns of Table 2), the best point achieved is given in the 6th and 7th columns of Table 2 with $\chi^2 \approx 1.491$ and $\sigma_{\max} \approx 0.501$. Lastly, we collect all points with maximum deviations ($\sigma_{\max} \leq 1$) to generate mean and spread values, given in the 8th and 9th columns of Table 2 with $\chi^2 \approx 1.895$. These values show the location and the size of the area with deviations from experimental values less than one (green area in Figure 5).

The masses and mixing angles in Table 2 were defined as eigenvalues of mass matrices in equations (18a), (19), and equation (21) for V^W_{CKM}, $V^{W'^{\pm}}$, and $V^{W'^0}$ mixing matrices, respectively.

Figure 5 summarizes all the data points collected according to two criteria: the horizontal axis corresponds to $\sigma_{\max}$ which represents the maximum deviation of each point with respect to the experimental value, and the vertical axis shows the χ^2 values for each point obtained. The plot is divided into three horizontal regions according to the value of $\sigma_{\max}$: 0-1, 1-2, and 2-3; the vertical region is separated into three categories as well, according to the values of $\langle\sigma\rangle/\sigma_{\max}$: 0–0.4, 0.4–0.6, and 0.6–1.0. This last category represents the spread of all errors that contribute to the total χ^2. The solid curves on the plot stand for the upper and lower theoretical limits for this plot given by $\chi^2 = 9\sigma^2_{\max}$ and $\chi^2 = \sigma^2_{\max}$, respectively.

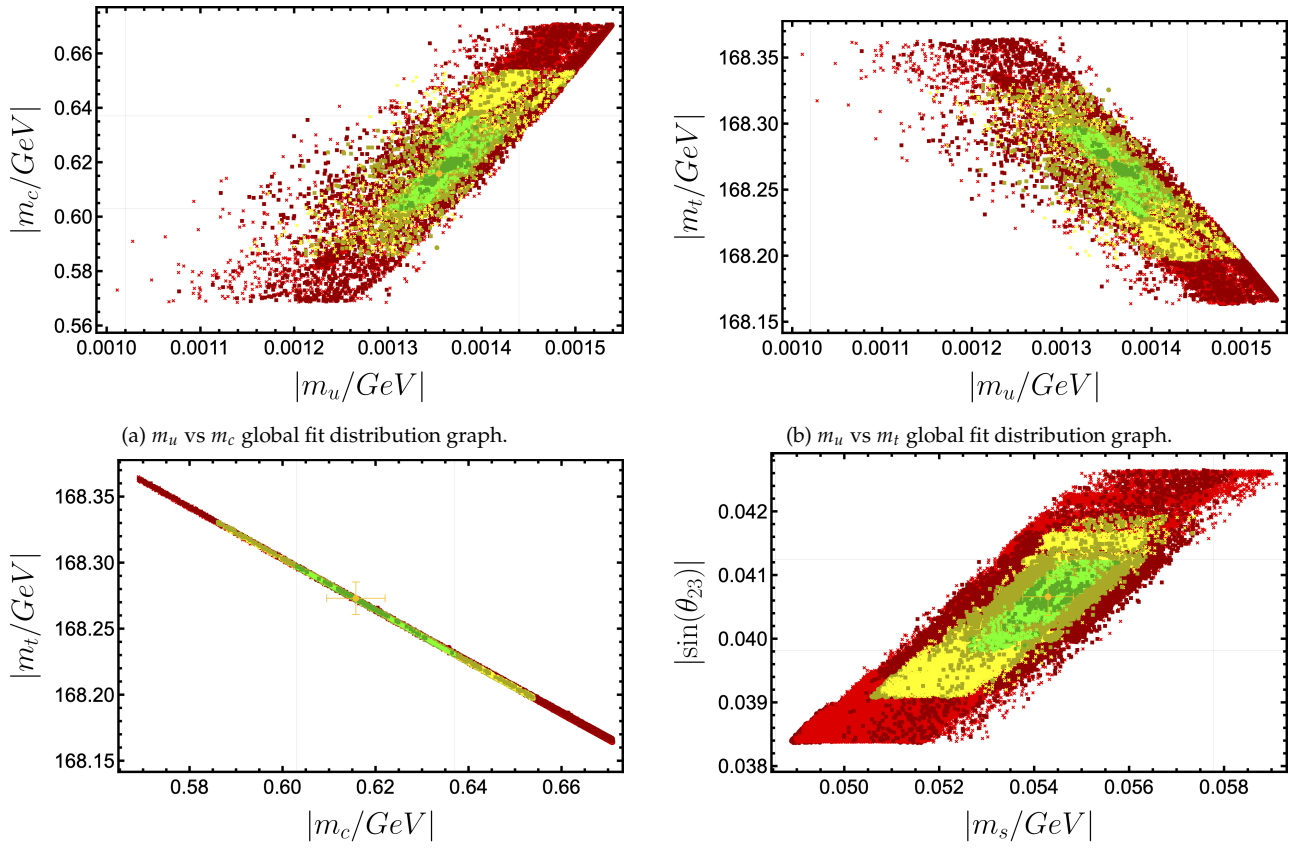

(a) m_u vs m_c global fit distribution graph.

(b) m_u vs m_t global fit distribution graph.

(c) m_c vs m_t global fit distribution graph.

(d) m_s vs $\sin(\theta_{23}^{\rm CKM})$ global fit distribution graph.

FIGURE 4: Selected observable correlation plots. Grid lines indicate a one standard deviation region of the experimental data. Green, yellow, and red colors stand for $\sigma_{\rm max} < 1$, 2, and 3, respectively, whereas squares, crosses, and discs correspond to $\langle\sigma\rangle/\sigma_{\rm max}$: 0–0.4, 0.4–0.6, and 0.6–1.0, respectively.

par.	BP1	BP2	BP3$_{\langle\rangle}$	BP3$_{\rm spread}$
β_u	−0.008127116503406678	−0.008074064951393775	−0.0081294	0.0000816256
γ_u	0.00012023151170229749	0.00012095573963901077	0.000120017	0.0000018874
β_d	0.044756546016957506	0.04508573236580676	0.0447492	0.000416564
γ_d	0.002037220066695815	0.0020439360347433004	0.00203794	0.0000212662
β_D	0.04796738067655066	0.04787190321609066	−0.0474458	0.000806016
γ_D	−0.05988836055185294	−0.06057801433337951	0.0605905	0.00131765
ε	1.0080400994427337	1.0080578648812581	1.00563	0.00575238

TABLE 1: Model input parameters for the several benchmark points given in Table 2.

6. DISCUSSION

One can isolate and determine the causes of different levels of correlation between parameters and observable variables in the plots given in the earlier section (Figures 2 and 4). Obviously, γ and β parameters affect mass values of quarks at up- and down-sector. Another factor in determining masses of the SM down-sector quarks is the existence of BSM heavy isosinglet quarks, hereafter the *BSM effect*. For example, one would expect that γ_u correlates with m_u strongly, and m_c and m_t weakly. However, since β_u is about 80 times greater than γ_u, a strong correlation of γ_u-m_u is smeared into the medium level through the interference of β_u. As expected, β_u correlates strongly with m_c and m_t. Due to the relative size of β_u with respect to γ_u, it affects m_u weakly.

However, the situation is different in down-sector. Similar to the up-sector, γ_d correlates with m_d on the medium level. The correlation between γ_d and other down-quark mass eigenvalues (m_s and m_b) disappears due to the BSM effect. The correlation of β_d with m_d, m_s, and m_b is degraded proportional to the closeness to BSM quarks. Therefore, similarly to the up-quark sector, the weak correlation of β_d-m_d has disappeared due to a small BSM effect, whereas the expected strong correlation between β_d and m_s weakens down to the medium level due to the existence of the same BSM effect. Finally, the strong correlation of β_d-m_b has disappeared due to very strong mixing with BSM quarks.

There are no significant correlations between SM parameters and BSM observables. D, S, and B exhibit similar behavior with respect to β_u, γ_u, β_d, and γ_d parameters. M_D and M_S have direct linear dependence on γ_D as well as weaker dependences on β_D. On the other hand, strong correlations are observed between M_B and β_D, as well as between M_B and γ_D.

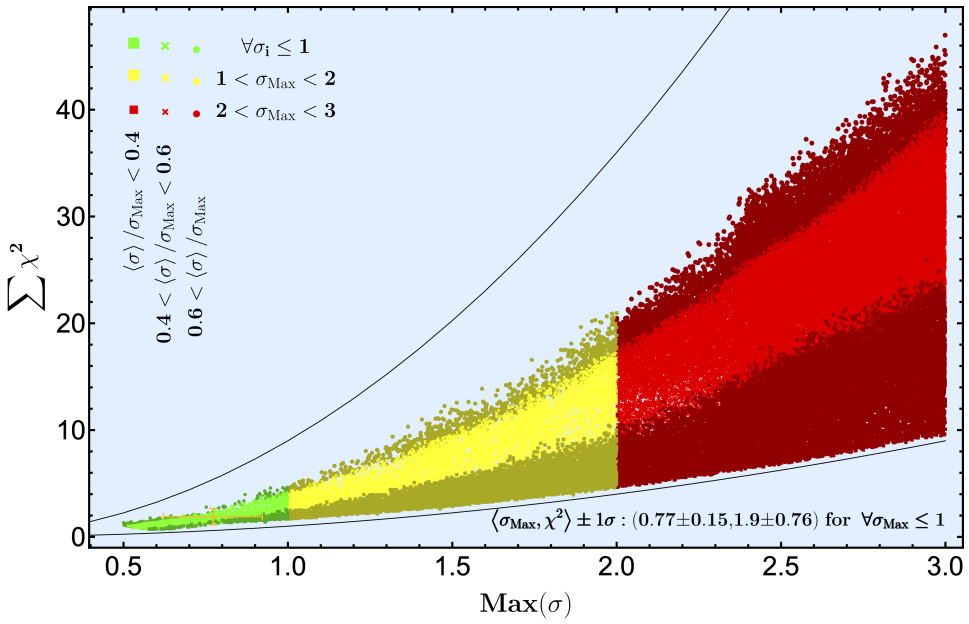

FIGURE 5: Model global fit vs maximum deviation (up to 3σ) distribution graph. The solid curves stand for upper and lower theoretical limits and $\langle\rangle$ stands for the mean value.

Observable	Experimental		BP1		BP2		BP3	
	Value	Err.	Value	σ	Value	σ	$\langle\rangle$	Spread
m_u (MeV)	1.23	0.21	1.35	0.59	1.33	0.50	1.35	0.02
m_c (MeV)	620	17	616	0.26	611	0.50	616	6
m_t (GeV)	168.26	0.75	168.27	0.018	168.28	0.028	168.27	0.01
m_d (MeV)	2.67	0.19	2.58	0.48	2.59	0.44	2.58	0.03
m_s (MeV)	53.16	4.61	54.33	0.25	54.81	0.36	54.29	0.53
m_b (GeV)	2.839	0.026	2.841	0.075	2.848	0.350	2.839	0.015
M_D (GeV)		—	8677	—	8790	—	8801	219
M_S (GeV)		—	9724	—	9824	—	9820	189
M_B (GeV)		—	96687	—	96710	—	96673	71
$\sin(\theta_{12})$	0.22650	0.000431	0.22653	0.071278	0.22671	0.48643	0.22649	0.000235
$\sin(\theta_{23})$	0.04053	$^{+0.000821}_{-0.000601}$	0.04066	0.18581	0.04086	0.47030	0.04066	0.000292
$\sin(\theta_{13})$	0.00361	$^{+0.000110}_{-0.000090}$	0.00359	0.15861	0.00364	0.30446	0.00359	0.000036
$\sin(\theta_{12}^{W'^{\pm}})$		—	0.67511	—	0.67502	—	0.67497	—
$\sin(\theta_{23}^{W'^{\pm}})$		—	0.06082	—	0.06112	—	0.04728	—
$\sin(\theta_{13}^{W'^{\pm}})$		—	0.00721	—	0.00693	—	0.00152	—
$\sin(\theta_{12}^{W'^{0}})$		—	0.82460	—	0.82462	—	0.82438	—
$\sin(\theta_{23}^{W'^{0}})$		—	0.03327	—	0.03345	—	0.07482	—
$\sin(\theta_{13}^{W'^{0}})$		—	0.02290	—	0.02335	—	0.02857	—
χ^2		—	0.777		1.491		1.895	

TABLE 2: Model various benchmark points with the smallest χ^2, smallest σ_{max}, and mean value for $\forall\sigma_{max} \leq 1$. Here, σ stands for standard deviation and has no units. The obtained values shown above were rounded to have the same significant figures as the experiment results.

As mentioned earlier, CP-violating phases are not considered in the present paper. Therefore, elements of mass matrices are chosen as real numbers. Consequently, some of the resulting eigenvalues of mass matrices and some elements of the CKM matrix are negative. It is possible to remove these negative signs and get correct CP-violating phases by including phase multipliers to democratic mass matrix elements. These multipliers may even help to pinpoint χ^2 and σ_{max}. The effect of the phases on the quark masses and CKM mixing angles is left for future works.

7. CONCLUSION

We have shown that the DMM mechanism might be valuable for different BSM models. Of course, if the chosen BSM model is the correct one, one should try to determine the underlying cause of small deviations to find this underlying theory for deviations. This would be a great achievement in the direction of understanding mass hierarchy.

Regarding the physical origin of the DMM pattern of the quark mass matrices, there are several possible approaches likely to establish the connection between DMM and underlying UV theory. The most common method found in literature is the use of discrete flavor symmetries, e.g., $\mathcal{A}_4$, see, for instance [92], which can be applied to lepton and/or quark sector mass

Quantity	ES1	ES2	ES3	ES4
$\frac{a_D \eta_D}{\sqrt{2}}$ (GeV)	2440	3454	5176	6899
ε	1.0081988	1.008152	1.0081097	1.008089
m_d (MeV)	2.59	2.52	2.51	2.50
m_s (MeV)	55.84	55.13	54.81	54.66
m_b (GeV)	2.838	2.840	2.840	2.841
M_D (GeV)	728	1000	1500	2000
M_S (GeV)	806	1118	1674	2231
M_B (GeV)	8029	11297	16840	22386
χ^2	1.82	2.63	2.69	2.72

TABLE 3: BSM energy scale scan (ES). In this scan, β and γ values are the same as in BP1. Therefore, one has the same CKM matrix elements, BSM CKM matrix elements, and up-sector masses as in BP1.

matrices. Use of global or gauged continuous symmetries (e.g., $U(1)_{\mu-\tau}$, $SU(3)$), so-called flat flavor symmetries, is another possibility. Also popular in recent years is the modular symmetries approach based on $\mathcal{A}_4, \mathcal{S}_4, \mathcal{A}_5$ [93, 94, 95, 96, 97, 98, 99] modular symmetries, where one can predict mass matrix patterns for leptons, and quarks as well [100, 101, 102]. The unique signature of modular symmetries is that the mixing angles, phases, and in some cases the SM fermion masses can be predicted from the theory.

In the present paper, the DMM approach is applied to the quark sector of the 331 model, which is inspired by E_6 symmetry. Model becomes prominent by being one of the simplest extensions of SM. Quark masses and mixing angles within one standard deviation of the experimental values with ten parameters are successfully derived. More specifically, each of the quark sectors (up, down, and isosinglet down) is controlled dominantly by set of three parameters (a, β, γ); additionally, one parameter corresponds to the mixing between SM and isosinglet down type quarks. In return, all SM and isosinglet quark masses and mixing angles are predicted, total of eighteen observable variables, nine out of which are SM variables.

Detailed analysis is performed in order to find the best fit benchmark point. The best fit point obtained has a $\chi^2 = 0.777$ with the largest standard deviation from the experimental values of 0.586 for m_u. Another important benchmark point is the point with the smallest achieved standard deviation error from the experimental data, $\chi^2 = 1.491$, and the largest deviation of 0.501. Furthermore, a summary data plot of $\sigma_{\max}$ vs χ^2 is produced, as well as the average point for all generated data with $\sigma_{\max} \leq 1$ condition.

Actually, it is possible to have a smaller mass for the D quark with a cost of χ^2 and $\sigma_{\max}$. For example, a relatively small value for $a_D \eta_D / \sqrt{2} = 2440\,\text{GeV}$ gives $m_D = 728\,\text{GeV}$ with $\chi^2 = 1.82$. So, it is possible even to be probed at the HL-LHC, FCC-hh, or some other future hadron collider (see [103] and references therein). An energy scale scan for various m_D masses is performed in Table 3.

The model at hand demonstrates that a democratic approach can successfully lead to the SM quark masses and hierarchy between them. Furthermore, CKM mixing angles are also obtained within corresponding experimental limits. This result motivates further exploration of parameter schemes based on fundamental democratic patterns. UV models of flavor symmetry leading naturally to democratic-based quark sector mass schemes should be studied in future works. From all of the above, it is concluded that this can be a possible explanation of the hierarchy problem.

Appendix A. CHIRAL GAUGE ANOMALY CANCELLATION

The chiral gauge anomaly cancellation, per generation, in the present model proceeds as follows:

$$[SU(3)_c]^2\, U(1)_X \;:\; 3X_Q + X_u + X_d + X_D = 0, \tag{A.1a}$$

$$[SU(3)_L]^2\, U(1)_X \;:\; 3X_Q + X_\Psi + X_{\Psi_1} + X_{\Psi_2} = 0, \tag{A.1b}$$

$$[U(1)_X]^3 \;:\; 9X_Q^3 + 3X_u^3 + 3X_d^3 + 3X_D^3 + 3X_\Psi^3 + 3X_{\Psi_1}^3 + 3X_{\Psi_3}^3 + \sum_l X_l^3, \tag{A.1c}$$

$$[\text{gravity}]^2 U(1)_X \;:\; 9X_Q + 3X_u + 3X_d + 3X_D + 3X_\Psi + 3X_{\Psi_1} + 3X_{\Psi_3} + \sum_l X_l, \tag{A.1d}$$

where l stands for leptonic singlets; their contribution to the chiral anomalies is zero and their presence in the model is not required.

Appendix B. QUARK MASS MATRICES AND RELATION BETWEEN YUKAWA AND $\beta_{u,d,D}, \gamma_{u,d,D}$ PARAMETERS

The complete form of the up-quark mass matrix is given by

$$\mathcal{M}_u^0 = \frac{\eta'}{\sqrt{2}} \begin{pmatrix} a_{uu} & a_{uc} & a_{ut} \\ a_{cu} & a_{cc} & a_{ct} \\ a_{tu} & a_{tc} & a_{tt} \end{pmatrix}. \tag{B.2}$$

Then, comparing the above with equation (18a), we arrive at

$$a_{uu} = a_u\,(1 + \gamma_u)\,, \tag{B.3a}$$

$$a_{uc} = a_{cu} = a_u, \tag{B.3b}$$

$$a_{ut} = a_{tu} = a_u \left(1 - \frac{9}{2}\gamma_u + \beta_u\right), \tag{B.3c}$$

$$a_{cc} = a_u\,(1 - 2\gamma_u)\,, \tag{B.3d}$$

$$a_{ct} = a_{tc} = a_u\,(1 + 3\gamma_u + \beta_u)\,, \tag{B.3e}$$

$$a_{tt} = a_u\,(1 + 4\beta_u)\,, \tag{B.3f}$$

where we used $\eta^u = \eta'$. Similarly, for the down-quarks, using equatios (19), (18b), and (18c), we have the relation between the

Yukawa couplings and the parameterization parameters as

$$a_{dd} = a_d\,(1+\gamma_d)\,, \tag{B.4a}$$
$$a_{ds} = a_{sd} = a_d, \tag{B.4b}$$
$$a_{db} = a_{bd} = a_d\left(1-\frac{9}{2}\gamma_d+\beta_d\right), \tag{B.4c}$$
$$a_{ss} = a_d\,(1-2\gamma_d)\,, \tag{B.4d}$$
$$a_{sb} = a_{bs} = a_d\,(1+3\gamma_d+\beta_d)\,, \tag{B.4e}$$
$$a_{bb} = a_d\,(1+4\beta_d)\,, \tag{B.4f}$$
$$a_{dD} = \varepsilon_d a_d\,(1+\gamma_d)\,, \tag{B.4g}$$
$$a_{dS} = a_{sD} = \varepsilon_d a_d, \tag{B.4h}$$
$$a_{dB} = a_{bD} = \varepsilon_d a_d\left(1-\frac{9}{2}\gamma_d+\beta_d\right), \tag{B.4i}$$
$$a_{sS} = \varepsilon_d a_d\,(1-2\gamma_d)\,, \tag{B.4j}$$
$$a_{sB} = a_{bS} = \varepsilon_d a_d\,(1+3\gamma_d+\beta_d)\,, \tag{B.4k}$$
$$a_{bB} = \varepsilon_d a_d\,(1+4\beta_d)\,, \tag{B.4l}$$
$$a_{Dd} = \varepsilon_d a_D\,(1+\gamma_D)\,, \tag{B.4m}$$
$$a_{Sd} = a_{Ds} = \varepsilon_d a_D, \tag{B.4n}$$
$$a_{Bd} = a_{Db} = \varepsilon_d a_D\left(1-\frac{9}{2}\gamma_D+\beta_D\right), \tag{B.4o}$$
$$a_{Ss} = \varepsilon_d a_D\,(1-2\gamma_D)\,, \tag{B.4p}$$
$$a_{Bs} = a_{Sb} = \varepsilon_d a_D\,(1+3\gamma_D+\beta_D)\,, \tag{B.4q}$$
$$a_{Bb} = \varepsilon_d a_D\,(1+4\beta_D)\,, \tag{B.4r}$$
$$a_{DD} = a_D\,(1+\gamma_D)\,, \tag{B.4s}$$
$$a_{SD} = a_{DS} = a_D, \tag{B.4t}$$
$$a_{BD} = a_{DB} = a_D\left(1-\frac{9}{2}\gamma_D+\beta_D\right), \tag{B.4u}$$
$$a_{SS} = a_D\,(1-2\gamma_D)\,, \tag{B.4v}$$
$$a_{BS} = a_{SB} = a_D\,(1+3\gamma_D+\beta_D)\,, \tag{B.4w}$$
$$a_{BB} = a_D\,(1+4\beta_D)\,, \tag{B.4x}$$

where $\eta^d = \eta$ and $\eta^D/\sqrt{2} = M$ was used.

Appendix C. EXTENDED CKM MATRIX AND UNITARITY

Extended CKM should be considered with extra care since it is (3×6) matrix as seen from the following argument:

$$V_{\rm CKM} = U_{uL}^{3\times 3} U_{dL}^{\dagger 3\times 6}, \tag{C.5a}$$
$$U_{dL}^{6\times 6} \to U_{dL} U_{dL}^{\dagger} = U_{dL}^{\dagger} U_{dL} = I_{6\times 6}, \tag{C.5b}$$
$$V_{\rm CKM} V_{\rm CKM}^{\dagger} = U_{uL}^{3\times 3} U_{dL}^{\dagger 3\times 6} U_{dL}^{6\times 3} U_{uL}^{3\times 3\dagger} = U_{uL}^{3\times 3} U_{uL}^{3\times 3\dagger} = I_{3\times 3}, \tag{C.5c}$$
$$V_{\rm CKM}^{\dagger} V_{\rm CKM} = U_{dL}^{6\times 3} U_{uL}^{3\times 3\dagger} U_{uL}^{3\times 3} U_{dL}^{\dagger 3\times 6} = U_{dL}^{6\times 3} U_{dL}^{\dagger 3\times 6} \neq I_{6\times 6}, \tag{C.5d}$$
$$U_{dL}^{\dagger 3\times 6} U_{dL}^{6\times 3} = I_{3\times 3} \text{ but } U_{dL}^{6\times 3} U_{dL}^{\dagger 3\times 6} \neq I_{6\times 6}. \tag{C.5e}$$

However, it is more conventional to deal with it with square matrices. Therefore, after extending (tensor multiplying with 2 dimensional unity matrix) the up-sector mixing matrix, with proper normalization, we recover the unitarity of the extended CKM matrix of the SM (see equation (C.6)).

$$\begin{aligned} V_{\rm CKM}^{6\times 6} &= \frac{1}{\sqrt{2}}\left(U_{uL}^{3\times 3}\otimes I_{2\times 2}\right) U_{dL}^{6\times 6} \\ &= \frac{1}{\sqrt{2}}\begin{pmatrix} U_{uL}^{3\times 3} & 0 \\ 0 & U_{uL}^{3\times 3}\end{pmatrix} U_{dL}^{6\times 6}. \end{aligned} \tag{C.6}$$

With the use of the duplication of up sector diagonalizing matrix, one obtains (6×6) extended CKM matrix for the benchmark point 1 as follows:

$$V_{\rm CKM}^{6\times 6} = \begin{array}{c} \begin{matrix} d & s & b & D & S & B \end{matrix} \\ \begin{pmatrix} 0.686 & -0.160 & -0.00253 & 0.0000644 & 0.0000558 & 0.00000668 \\ 0.159 & 0.685 & 0.0286 & -0.000335 & -0.000164 & -0.0000748 \\ 0.00402 & 0.0285 & -0.704 & 0.000455 & -0.000614 & 0.00184 \\ -0.691 & 0.161 & 0.00255 & -0.738 & -0.674 & -0.0357 \\ -0.161 & -0.691 & -0.0289 & 0.675 & 0.736 & -0.0497 \\ -0.00406 & -0.0287 & 0.709 & 0.00679 & -0.0601 & 0.998 \end{pmatrix} \end{array} \begin{matrix} u \\ c \\ t \\ u \\ c \\ t \end{matrix} \tag{C.7}$$

Because of the duplication, there are two V_{ud} values. Both of these values are affected form ε at certain levels. As an example, to obtain the correct value for V_{ud}, one should include both values in equation (C.7) as follows:

$$V_{ud} = \sqrt{0.686^2 + (-0.691)^2} = 0.974. \tag{C.8}$$

When we remove all the duplication on extended CKM by using the procedure in equation (C.8), it is possible to obtain (3×6) CKM matrix as follows:

$$V_{\rm CKM}^{3\times 6} = \begin{array}{c} \begin{matrix} d & s & b & \vdots & D & S & B \end{matrix} \\ \begin{pmatrix} 0.9740 & 0.2265 & 0.00360 & \vdots & 0.738 & 0.674 & 0.0357 \\ 0.22647 & 0.9732 & 0.0407 & \vdots & 0.675 & 0.736 & 0.0497 \\ 0.00571 & 0.0404 & 0.99917 & \vdots & 0.00680 & 0.0601 & 0.998 \end{pmatrix} \end{array} \begin{matrix} u \\ c \\ t \end{matrix} \tag{C.9}$$

The first 3×3 part of the $V_{\text{CKM}}^{3\times6}$ correspond to standard model CKM matrix and it is inherently satisfying unitarity conditions. The second 3×3 part of the $V_{\text{CKM}}^{3\times6}$ correspond to the BSM analog of the conventional CKM matrix, also separately satisfying the unitarity conditions. This is possible because heavy quarks decay through processes similar to $D \to uW'^{-}$.

CONFLICTS OF INTEREST

The authors declare that there are no conflicts of interest regarding the publication of this paper.

ACKNOWLEDGMENTS

Rena Çiftçi was supported by the Ege University Scientific Research Projects Coordination under Grant Number FGA-2021-22954. Oleg Popov was supported in part by the National Natural Science Fund of China Grant No. 12350410373 and in part by the Samsung Science and Technology Foundation under Grant No. SSTF-BA1602-04 and National Research Foundation of Korea under Grant Number 2018R1A2B6007000.

References

[1] N. T. Duy, P. N. Thu, and D. T. Huong. New physics in b $\to$ s transitions in the MF331 model. 5 2022.

[2] Andrea Addazi, Giulia Ricciardi, Simone Scarlatella, Rahul Srivastava, and José W. F. Valle. An old theme for new data: Interpreting recent B anomaly data within an extended 331 gauge theory. 1 2022.

[3] Andrzej J. Buras, Fulvia De Fazio, and Jennifer Girrbach. 331 models facing new $b \to s\mu^+\mu^-$ data. *JHEP*, 02:112, 2014.

[4] Andrzej J. Buras, Fulvia De Fazio, Jennifer Girrbach, and Maria V. Carlucci. The Anatomy of Quark Flavour Observables in 331 Models in the Flavour Precision Era. *JHEP*, 02:023, 2013.

[5] Sofiane M. Boucenna, Stefano Morisi, and Jose W. F. Valle. Radiative neutrino mass in 3-3-1 scheme. *Phys. Rev. D*, 90(1):013005, 2014.

[6] M. B. Tully and Girish C. Joshi. Generating neutrino mass in the 331 model. *Phys. Rev. D*, 64:011301, 2001.

[7] M. Singer, J. W. F. Valle, and J. Schechter. Canonical Neutral Current Predictions From the Weak Electromagnetic Gauge Group $SU(3) \times U(1)$. *Phys. Rev. D*, 22:738, 1980.

[8] F. Pisano and V. Pleitez. An $SU(3) \times U(1)$ model for electroweak interactions. *Phys. Rev. D*, 46:410–417, 1992.

[9] P. H. Frampton. Chiral dilepton model and the flavor question. *Phys. Rev. Lett.*, 69:2889–2891, 1992.

[10] Mario Reig, José W. F. Valle, and C. A. Vaquera-Araujo. Unifying left–right symmetry and 331 electroweak theories. *Phys. Lett. B*, 766:35–40, 2017.

[11] Hoang Ngoc Long. The 331 model with right handed neutrinos. *Phys. Rev. D*, 53:437–445, 1996.

[12] A. E. Carcamo Hernandez, R. Martinez, and F. Ochoa. Z and Z' decays with and without FCNC in 331 models. *Phys. Rev. D*, 73:035007, 2006.

[13] James T. Liu and Daniel Ng. Lepton flavor changing processes and CP violation in the 331 model. *Phys. Rev. D*, 50:548–557, 1994.

[14] Stefano Profumo and Farinaldo S. Queiroz. Constraining the Z' mass in 331 models using direct dark matter detection. *Eur. Phys. J. C*, 74(7):2960, 2014.

[15] Antonio Enrique Cárcamo Hernández, R. Martinez, and F. Ochoa. Fermion masses and mixings in the 3-3-1 model with right-handed neutrinos based on the S_3 flavor symmetry. *Eur. Phys. J. C*, 76(11):634, 2016.

[16] Renato M. Fonseca and Martin Hirsch. A flipped 331 model. *JHEP*, 08:003, 2016.

[17] T. Aaltonen et al. High-precision measurement of the W boson mass with the CDF II detector. *Science*, 376(6589):170–176, 2022.

[18] M. C. Rodriguez. The W-boson mass anomaly and Supersymmetric $SU(3)_C \otimes SU(3)_L \otimes U(1)_N$ Model. 5 2022.

[19] A. E. Carcamo Hernandez, R. Martinez, and F. Ochoa. Radiative seesaw-type mechanism of quark masses in $SU(3)_C \otimes SU(3)_L \otimes U(1)_X$. *Phys. Rev. D*, 87(7):075009, 2013.

[20] A. E. Cárcamo Hernández, E. Cataño Mur, and R. Martinez. Lepton masses and mixing in $SU(3)_C \otimes SU(3)_L \otimes U(1)_X$ models with a S_3 flavor symmetry. *Phys. Rev. D*, 90(7):073001, 2014.

[21] A. E. Cárcamo Hernández, Sergey Kovalenko, H. N. Long, and Ivan Schmidt. A variant of 3-3-1 model for the generation of the SM fermion mass and mixing pattern. *JHEP*, 07:144, 2018.

[22] E. R. Barreto, A. G. Dias, J. Leite, C. C. Nishi, R. L. N. Oliveira, and W. C. Vieira. Hierarchical fermions and detectable Z' from effective two-Higgs-triplet 3-3-1 model. *Phys. Rev. D*, 97(5):055047, 2018.

[23] Frank F. Deppisch, Chandan Hati, Sudhanwa Patra, Utpal Sarkar, and Josè W. F. Valle. 331 Models and Grand Unification: From Minimal SU(5) to Minimal SU(6). *Phys. Lett. B*, 762:432–440, 2016.

[24] Corey Kownacki, Ernest Ma, Nicholas Pollard, Oleg Popov, and Mohammadreza Zakeri. Dark revelations of the $[SU(3)]^3$ and $[SU(3)]^4$ gauge extensions of the standard model. *Phys. Lett. B*, 777:121–124, 2018.

[25] Corey Kownacki, Ernest Ma, Nicholas Pollard, Oleg Popov, and Mohammadreza Zakeri. Alternative $[SU(3)]^4$ model of leptonic color and dark matter. *Nucl. Phys. B*, 928:520–534, 2018.

[26] Alexandre Alves, Giorgio Arcadi, P. V. Dong, Laura Duarte, Farinaldo S. Queiroz, and José W. F. Valle. Matter-parity as a residual gauge symmetry: Probing a theory of cosmological dark matter. *Phys. Lett. B*, 772:825–831, 2017.

[27] P. V. Dong, D. T. Huong, Farinaldo S. Queiroz, José W. F. Valle, and C. A. Vaquera-Araujo. The Dark Side of Flipped Trinification. *JHEP*, 04:143, 2018.

[28] Sin Kyu Kang, Oleg Popov, Rahul Srivastava, José W. F. Valle, and Carlos A. Vaquera-Araujo. Scotogenic dark matter stability from gauged matter parity. *Phys. Lett. B*, 798:135013, 2019.

[29] Julio Leite, Oleg Popov, Rahul Srivastava, and José W. F. Valle. A theory for scotogenic dark matter stabilised by residual gauge symmetry. *Phys. Lett. B*, 802:135254, 2020.

[30] Harald Fritzsch, Zhi-zhong Xing, and Di Zhang. Correlations between quark mass and flavor mixing hierarchies. *Nucl. Phys. B*, 974:115634, 2022.

[31] P.A. Zyla et al. Review of Particle Physics. *PTEP*, 2020(8):083C01, 2020. and 2021 update.

[32] G. Dattoli and E. Di Palma. The exponential parameterization of the quark mixing matrix. 1 2013.

[33] G. C. Branco and L. Lavoura. Wolfenstein Type Parametrization of the Quark Mixing Matrix. *Phys. Rev. D*, 38:2295, 1988.

[34] Werner Rodejohann. Unified Parametrization for Quark and Lepton Mixing Angles. *Phys. Lett. B*, 671:267–271, 2009.

[35] Xiao-Gang He, Shi-Wen Li, and Bo-Qiang Ma. Triminimal Parametrization of Quark Mixing Matrix. *Phys. Rev. D*, 78:111301, 2008.

[36] Shi-Wen Li and Bo-Qiang Ma. Unified parametrization of quark and lepton mixing matrices in tri-bimaximal pattern. *Phys. Rev. D*, 77:093005, 2008.

[37] S. Chaturvedi, V. Gupta, G. Sanchez-Colon, and N. Mukunda. Recursive parametrization of Quark flavour mixing matrices. *Rev. Mex. Fis.*, 57:146–153, 2011.

[38] G. C. Branco and L. Lavoura. Rephasing Invariant Parametrization of the Quark Mixing Matrix. *Phys. Lett. B*, 208:123–130, 1988.

[39] Nan Li and Bo-Qiang Ma. Unified parametrization of quark and lepton mixing matrices. *Phys. Rev. D*, 71:097301, 2005.

[40] S. Chaturvedi and Virendra Gupta. Parametrization of the quark mixing matrix involving its eigenvalues. *AIP Conf. Proc.*, 670(1):73–80, 2003.

[41] Joy Ganguly. Fermion mass hierarchy and lepton flavor violation using *CP* symmetry. 5 2022.

[42] Haim Harari, Hervé Haut, and Jacques Weyers. Quark masses and cabibbo angles. *Physics Letters B*, 78(4):459–461, 1978.

[43] Harald Fritzsch. Quark masses and flavor mixing. *Nuclear Physics B*, 155(1):189–207, 1979.

[44] Harald Fritzsch. Hierarchical chiral symmetries and the quark mass matrix. *Physics Letters B*, 184(4):391–396, 1987.

[45] H. Fritzsch and J. Plankl. Flavour democracy and the lepton-quark hierarchy. *Physics Letters B*, 237(3):451–456, 1990.

[46] Harald Fritzsch and Dirk Holtmannspötter. The breaking of subnuclear democracy as the origin of flavour mixing. *Physics Letters B*, 338(2):290–294, 1994.

[47] Amitava Datta and Sreerup Raychaudhuri. Quark masses and mixing angles in a four-generation model with a naturally heavy neutrino. *Phys. Rev. D*, 49:4762–4772, May 1994.

[48] A. Çelikel, A. K. Çiftçi, and S. Sultansoy. A search for the fourth SM family. *Physics Letters B*, 342(1):257–261, 1995.

[49] S. Atağ, A. Çelikel, A. K. Çiftçi, S. Sultansoy, and Ü. O. Yilmaz. Fourth SM family, breaking of mass democracy, and the CKM mixings. *Phys. Rev. D*, 54:5745–5749, Nov 1996.

[50] A. K. Çiftçi, R. Çiftçi, and S. Sultansoy. Search for the fourth standard model family fermions and E_6 quarks at $\mu^+\mu^-$ colliders. *Phys. Rev. D*, 65:055001, Jan 2002.

[51] A. K. Çiftçi, R. Çiftçi, and S. Sultansoy. Fourth standard model family neutrino at future linear colliders. *Phys. Rev. D*, 72:053006, Sep 2005.

[52] Abdelhak Djouadi and Alexander Lenz. Sealing the fate of a fourth generation of fermions. *Physics Letters B*, 715(4):310–314, 2012.

[53] C Collaboration, Suzan Basegmez, Giacomo Bruno, Roberto Castello, Ludivine Ceard, Christophe Delaere, Tristan Du Pree, Denis Favart, Laurent Forthomme, Andrea Giammanco, et al. Searches for higgs bosons in pp collisions at $\sqrt{s}$= 7 and 8 TeV in the context of four-generation and fermiophobic models. *Phys. Lett*, 725:36–59, 2013.

[54] K. T. Mahanthappa and P. K. Mohapatra. AN UNUNIFIABLE EXTRA U(1). *Phys. Rev. D*, 42:2400–2403, 1990.

[55] F. Gursey, Pierre Ramond, and P. Sikivie. A Universal Gauge Theory Model Based on E6. *Phys. Lett. B*, 60:177–180, 1976.

[56] Pierre Ramond. Calculable Masses in GUTS: An E_6 Example. *AIP Conf. Proc.*, 72:467–474, 1981.

[57] Carl H. Albright, C. Jarlskog, and M. O. Tjia. Implications of Gauge Theories for Heavy Leptons. *Nucl. Phys. B*, 86:535–547, 1975.

[58] K. T. Mahanthappa and P. K. Mohapatra. Limits on mixing angle and mass of Z-prime using Delta rho and atomic parity violation. *Phys. Rev. D*, 43:3093, 1991. [Erratum: Phys.Rev.D 44, 1616 (1991)].

[59] K. T. Mahanthappa and P. K. Mohapatra. Effects of Extra U(1)*s* in $SU(3)_l \times U(1)$ and Other Models. *Phys. Rev. D*, 42:1732–1737, 1990.

[60] M. Singer. An $SU(3) \times U(1)$ Theory of Weak Electromagnetic Interactions With Charged Boson Mixing. *Phys. Rev. D*, 19:296, 1979.

[61] R. Michael Barnett and Lay Nam Chang. The Source of Trimuon Events in Neutrino Scattering. *Phys. Lett. B*, 72:233–236, 1977.

[62] D. Horn and Graham G. Ross. Trimuons in SU(3) Gauge Models. *Phys. Lett. B*, 69:364–368, 1977.

[63] Paul Langacker and Gino Segre. Heavy Leptons and Trimuons in an $SU(3) \times U(1)$ Model. *Phys. Rev. Lett.*, 39:259, 1977.

[64] Benjamin W. Lee and Steven Weinberg. $SU(3) \times U(1)$ Gauge Theory of the Weak and Electromagnetic Interactions. *Phys. Rev. Lett.*, 38:1237, 1977.

[65] Motohiko Yoshimura. Vector-Like $SU(3) \times U(1)$ Gauge Model. *Prog. Theor. Phys.*, 57:237, 1977.

[66] G. Segre and J. Weyers. A Vector-Like Theory with a Parity Violating Neutral Current and Natural Symmetry. *Phys. Lett. B*, 65:243–245, 1976.

[67] Pierre Ramond. Unified Theory of Strong, Electromagnetic, and Weak Interactions Based on the Vector-Like Group E(7). *Nucl. Phys. B*, 110:214–228, 1976.

[68] F. Gursey and P. Sikivie. E(7) as a Universal Gauge Group. *Phys. Rev. Lett.*, 36:775, 1976.

[69] H. Fritzsch and P. Minkowski. SU(3) as Gauge Group of the Vector-Like Weak and Electromagnetic Interactions. *Phys. Lett. B*, 63:99–103, 1976.

[70] Pierre Fayet. A Gauge Theory of Weak and Electromagnetic Interactions with Spontaneous Parity Breaking. *Nucl. Phys. B*, 78:14–28, 1974.

[71] D. Gomez Dumm. Leptophobic character of the Z-prime in an $SU(3)_C \times SU(3)_L \times U(1)_X$ model. *Phys. Lett. B*, 411:313–320, 1997.

[72] Murat Ozer. $SU(3)_L \times U(1)_X$ model of the electroweak interactions without exotic quarks. *Phys. Rev. D*, 54:1143–1149, 1996.

[73] Murat Ozer. GIM mechanism and its consequences in the $SU(3)_L \times U(1)_X$ models of electroweak interactions.

Phys. Rev. D, 54:4561–4565, 1996.

[74] L. Epele, H. Fanchiotti, C. Garcia Canal, and D. Gomez Dumm. Spontaneous CP violation in an $SU(3)_L \times U(1)_Y$ electroweak model. *Phys. Lett. B*, 343:291–294, 1995.

[75] Daniel Ng. The Electroweak theory of $SU(3) \times U(1)$. *Phys. Rev. D*, 49:4805–4811, 1994.

[76] V. Pleitez and M. D. Tonasse. Neutrinoless double beta decay in an $SU(3)_L \times U(1)_N$ model. *Phys. Rev. D*, 48:5274–5279, 1993.

[77] J. C. Montero, F. Pisano, and V. Pleitez. Neutral currents and GIM mechanism in $SU(3)_L \times U(1)_N$ models for electroweak interactions. *Phys. Rev. D*, 47:2918–2929, 1993.

[78] V. Pleitez and M. D. Tonasse. Heavy charged leptons in an $SU(3)_L \times U(1)_N$ model. *Phys. Rev. D*, 48:2353–2355, 1993.

[79] Robert Foot, Oscar F. Hernandez, F. Pisano, and V. Pleitez. Lepton masses in an $SU(3)_L \times U(1)_N$ gauge model. *Phys. Rev. D*, 47:4158–4161, 1993.

[80] Hoang Ngoc Long. $SU(3)_L \times U(1)_N$ model for right-handed neutrino neutral currents. *Phys. Rev. D*, 54:4691–4693, 1996.

[81] Vicente Pleitez. New fermions and a vector - like third generation in $SU(3)_C \times SU(3)_L \times U(1)_N$ models. *Phys. Rev. D*, 53:514–526, 1996.

[82] H. N. Long, L. T. Hue, and D. V. Loi. Electroweak theory based on SU(4)$_L$⊗U(1)$_X$ gauge group. *Phys. Rev. D*, 94(1):015007, 2016.

[83] Soumia Lebbal, Jamal Mimouni, and Noureddine Mebarki. A 331 model for Lepton Flavor Universality Violation in B decays. *Int. J. Mod. Phys. A*, 37(02):2250005, 2022.

[84] Sébastien Descotes-Genon, Marta Moscati, and Giulia Ricciardi. Nonminimal 331 model for lepton flavor universality violation in $b \to s\ell\ell$ decays. *Phys. Rev. D*, 98(11):115030, 2018.

[85] William A. Ponce, Juan B. Florez, and Luis A. Sanchez. Analysis of $SU(3)_c \times SU(3)_L \times U(1)_X$ local gauge theory. *Int. J. Mod. Phys. A*, 17:643–660, 2002.

[86] Luis A. Sanchez, William A. Ponce, and R. Martinez. $SU(3)_c \times SU(3)_\ell \times U(1)_X$ as an E(6) subgroup. *Phys. Rev. D*, 64:075013, 2001.

[87] R. Martinez, William A. Ponce, and Luis A. Sanchez. $SU(3)_C \times SU(3)_L \times U(1)_X$ as an $SU(6) \times U(1)_X$ subgroup. *Phys. Rev. D*, 65:055013, 2002.

[88] Andre Nepomuceno and Bernhard Meirose. Limits on 331 vector bosons from LHC proton collision data. *Phys. Rev. D*, 101(3):035017, 2020.

[89] D. Cogollo, F. F. Freitas, C. A. de S. Pires, Yohan M. Oviedo-Torres, and P. Vasconcelos. Deep learning analysis of the inverse seesaw in a 3-3-1 model at the LHC. *Phys. Lett. B*, 811:135931, 2020.

[90] G. Aad, B. Abbott, D. C. Abbott, O. Abdinov, A. Abed Abud, K. Abeling, and D. K. Abhayasinghe. Search for a heavy charged boson in events with a charged lepton and missing transverse momentum from pp collisions at $\sqrt{s} = 13$ TeV with the atlas detector. *Phys. Rev. D*, 100:052013, Sep 2019.

[91] R. Çiftçi and A. K. Çiftçi. General structure of democratic mass matrix of quark sector in E_6 model. *AIP Conf. Proc.*, 1722(1):070004, 2016.

[92] Salvador Centelles Chuliá, Rahul Srivastava, and José W. F. Valle. Generalized Bottom-Tau unification, neutrino oscillations and dark matter: predictions from a lepton quarticity flavor approach. *Phys. Lett. B*, 773:26–33, 2017.

[93] Ferruccio Feruglio. *Are neutrino masses modular forms?*, pages 227–266. 2019.

[94] Takaaki Nomura, Hiroshi Okada, and Oleg Popov. A modular A_4 symmetric scotogenic model. *Phys. Lett. B*, 803:135294, 2020.

[95] Arnab Dasgupta, Takaaki Nomura, Hiroshi Okada, Oleg Popov, and Morimitsu Tanimoto. Dirac Radiative Neutrino Mass with Modular Symmetry and Leptogenesis. 11 2021.

[96] J. T. Penedo and S. T. Petcov. Lepton Masses and Mixing from Modular S_4 Symmetry. *Nucl. Phys. B*, 939:292–307, 2019.

[97] P. P. Novichkov, J. T. Penedo, S. T. Petcov, and A. V. Titov. Modular A_5 symmetry for flavour model building. *JHEP*, 04:174, 2019.

[98] Francisco J. de Anda, Stephen F. King, and Elena Perdomo. $SU(5)$ grand unified theory with A_4 modular symmetry. *Phys. Rev. D*, 101(1):015028, 2020.

[99] Gui-Jun Ding, Stephen F. King, and Xiang-Gan Liu. Neutrino mass and mixing with A_5 modular symmetry. *Phys. Rev. D*, 100(11):115005, 2019.

[100] Jun-Nan Lu, Xiang-Gan Liu, and Gui-Jun Ding. Modular symmetry origin of texture zeros and quark lepton unification. *Phys. Rev. D*, 101(11):115020, 2020.

[101] Hiroshi Okada and Morimitsu Tanimoto. Quark and lepton flavors with common modulus τ in A_4 modular symmetry. 5 2020.

[102] Chang-Yuan Yao, Jun-Nan Lu, and Gui-Jun Ding. Modular Invariant A_4 Models for Quarks and Leptons with Generalized CP Symmetry. *JHEP*, 05:102, 2021.

[103] João M. Alves, G. C. Branco, A. L. Cherchiglia, C. C. Nishi, J. T. Penedo, Pedro M. F. Pereira, M. N. Rebelo, and J. I. Silva-Marcos. Vector-like singlet quarks: A roadmap. *Phys. Rept.*, 1057:1–69, 2024.